



DEGREE PROJECT IN MATHEMATICS,  
SECOND CYCLE, 30 CREDITS  
*STOCKHOLM, SWEDEN 2016*

# **Velocity estimation in land vehicle applications**

Sensor Fusion using GPS, IMU and Output-shaft

**CHRISTIAN JONSSON**

KTH ROYAL INSTITUTE OF TECHNOLOGY  
SCHOOL OF ENGINEERING SCIENCES



# Velocity estimation in land vehicle applications

Sensor Fusion using GPS, IMU and Output-shaft

C H R I S T I A N J O N S S O N

Master's Thesis in Systems Engineering (30 ECTS credits)  
Degree Programme in Aerospace Engineering (120 credits)  
Royal Institute of Technology year 2016  
Supervisors at Scania: Agnes Johansson and Alfred Johansson  
Supervisor at KTH: Per Engvist  
Examiner: Per Engvist

TRITA-MAT-E 2016:31  
ISRN-KTH/MAT/E--16/31--SE

Royal Institute of Technology  
*SCI School of Engineering Sciences*

**KTH SCI**  
SE-100 44 Stockholm, Sweden

URL: [www.kth.se/sci](http://www.kth.se/sci)



# Abstract

In this project an alternative velocity-signal for Scania's heavy-duty vehicles was investigated. The current velocity estimation is based on wheel-encoders obtained from other control-units like ABS- and EBS-systems. Furthermore the wheel-encoders may have poor properties at both high and low velocities. Because the velocity is important for the automatic manual gear-switching sequence, Opticruise used in Scania transmission management system (TMS), an alternative velocity estimation based only on the internal signals in the TMS and GPS is desirable.

In this project the proposed algorithm utilizes sensor-fusion of a GPS, the rotational-velocity from the Output-shaft and an inertial measurement unit (IMU). An external 6-axis IMU, consisting of accelerometers and gyroscopes, was implemented to investigate if a more complete sensor-configuration would have potential benefits compared to the reduced 2-axis IMU currently in the TMS. The sensor-fusion algorithms are based on two different state-observers: Sliding mode observer (SMO), and Extended Kalman filter(EKF).

The two different sensor configurations had similar performance in good conditions. But the expanded sensor-configuration would outperformed the standard in critical-scenarios, where signals either becomes lost or bad. Other phenomenon like Coriolis-accelerations could be observed and compensated for with additional sensors, and in the process improve the velocity-estimation further. A method is also proposed to detect slippage in both the GPS or the Output-shaft, and compensate for a known constant delay. Resulting in a better velocity estimation compared to the current TMS velocity-estimation, based on tachometers from the wheels, during the scenarios considered in this project.



# Referat

## Hastighetsskattning av landfordon med GPS, IMU och utgående-axel

Det här projektet undersöktes en alternativ hastighetssignal till Scania's tunga lastbilar. Den nuvarande hastighetsuppskattningen är baserad på hjulsensorer från andra kontrollenheter, som ABS- och EBS-system, och kan ha dåliga egenskaper vid låga och höga hastigheter. Eftersom hastigheten är en viktig variabel till den Automatiserade växelsekvensen opticruise, som används i Scanias styrenhet för transmissionen (TMS), en alternativ metod för att estimera hastigheten som är enbart baserad på TMS interna signaler och GPS är därför önskvärd.

I detta projekt den föreslagna algoritmen utnyttjar sensorfusion av en GPS, rotationshastighet från den utgående axel, och en inertial measurement unit (IMU). En extern 6-axlig IMU, bestående av accelerometrar och gyroskop, implementerades för att undersöka om en mer komplett sensorkonfiguration har potentiella fördelar jämfört med den reducerade två-axlig IMU som nuvarande finns i TMS'en. Sensorfusionen är baserad på två olika observatörer: Sliding mode observer (SMO), och Extended Kalman filter (EKF).

De två olika sensorkonfigurationer hade liknande prestanda under goda förhållanden. Men den expanderade sensorkonfigurationen hade bättre egenskaper under kritiska scenarier, när signaler antingen förloras eller blir dåligt. Andra fenomen som Coriolis-accelerationer kunde observeras och kompenseras för med ytterligare sensorer.

Den föreslagna algoritmen kan också upptäcka avvikningar som slir i både GPS eller den utgående axel, och även kompensera för en latens i GPS-signalen. Detta resulterar i en bättre hastighetsuppskattning jämfört med nuvarande TMS hastighetsuppskattning baserat på hjulsatighetsensorer på de scenarion som undersökt i detta projekt.



# Contents

<b>1</b>	<b>Introduction and Background</b>	<b>3</b>
1.1	Problem Description . . . . .	3
1.2	Background . . . . .	3
1.3	Literature . . . . .	4
<b>2</b>	<b>Methods</b>	<b>7</b>
2.1	Sensor setup . . . . .	7
2.1.1	Sensor architecture . . . . .	7
2.1.2	Sensor model & System equations . . . . .	9
2.1.3	Unaligned sensors . . . . .	13
2.2	State equations . . . . .	15
2.3	Kalman filter . . . . .	15
2.4	Sliding mode observer . . . . .	17
2.4.1	Non-linear Sliding mode observer . . . . .	17
2.5	Fusing two redundant signals . . . . .	18
2.6	Testing, and Critical scenarios . . . . .	18
2.7	Slip detection . . . . .	20
2.8	Latency compensation . . . . .	21
<b>3</b>	<b>Results</b>	<b>23</b>
3.1	General characteristics of the signals, and results . . . . .	23
3.1.1	GPS . . . . .	23
3.1.2	Alignment of strap-down IMU . . . . .	24
3.1.3	Output-shaft . . . . .	25
3.2	Comparison Kalman vs. Sliding mode . . . . .	26
3.3	Improving the sensor configuration . . . . .	30
3.3.1	Coriolis . . . . .	33
3.4	Robustness . . . . .	36
3.4.1	GPS-outage . . . . .	36
3.4.2	Slip Detection . . . . .	37
3.4.3	Velocity extremes . . . . .	39
3.5	Delay compensation . . . . .	43

<b>4 Discussion and Conclusion</b>	<b>47</b>
4.1 Discussion . . . . .	47
4.2 Conclusion . . . . .	49
4.3 Future work and recommendations . . . . .	49
<b>Bibliography</b>	<b>51</b>
<b>Appendices</b>	<b>53</b>
<b>A Figures</b>	<b>55</b>
A.1 Logic constraints . . . . .	55
A.2 Coriolis . . . . .	56
<b>B Code</b>	<b>57</b>

# Nomenclature

$\omega_{x,y,z}$	The angular velocity measured by the different gyros, where x,y,z are the direction of the measurement.
$\phi$	The roll of the vehicle.
$\theta$	The pitch of the vehicle.
$a_{x,y,z}$	The acceleration measured by the different accelerometers, where x,y,z are the direction of the measurement.
<i>ABS</i>	Anti-lock breaking system
<i>CAN</i>	Controller Area Network
<i>CoR</i>	Centre of rotation
$e_k$	Error variable at the discrete time increment $k$
<i>EBS</i>	Electronic brake system
<i>EKF</i>	Extended Kalman filter
$g$	Gravitational constant
<i>GPS</i>	Global positioning unit
<i>IMU</i>	Inertial measuring unit
<i>MAE</i>	Mean absolute error
<i>MIMO</i>	Multiple input, multiple output
<i>NED</i>	Navigation-frame, where the letters represent the axis north, east, down
$P$	Is the error covariance matrix
$Q$	the covariance matrix associated with the model and the input noise

## CONTENTS

$R$	the covariance matrix of the measurement noise.
$TMS$	Transmission management system
$TMSWEE$	Transmission management systems wheel encoder based estimate
$v_k$	Measurement noise at the discrete time increment $k$
$v_{x,y,z}$	The velocity of the vehicle, where x,y,z are the direction.
$vSen$	Virtual Sensors
$w_k$	State disturbance at the discrete time increment $k$
$WE$	Wheel encoders
$x_k$	State variable at the discrete time increment $k$
$y_k$	State measurement at the discrete time increment $k$

# **Chapter 1**

## **Introduction and Background**

### **1.1 Problem Description**

This project address the issue of estimating the velocity of a heavy duty vehicle using IMU and GPS. The aim of this project was to obtain a good estimation of the vehicle independent of the tachometer, ABS or EBS-systems, currently used today. The reason for this is that the wheel sensors are only reliable and give a good estimate after a certain speed. Thus the sensor setup needs to be adequately accurate at low speeds and give a good approximation of the true vehicular velocity. The velocity is important to decide which gears or the optimal gear sequence for the automated manual gearbox, Opticruise, used in Scania vehicles. In this industry oriented project there is incitement for modular systems, being independent from other control units other than the transmission management system(TMS). Therefore one of the aims of this project is to provide a robust real-time algorithm, and sensor setup to obtain accurate estimations of the velocity.

### **1.2 Background**

Scania's Automated manual gearbox uses Scania developed software Opticruise to obtain an optimal gear switching sequence. One of the key variables in this algorithm is velocity and it is crucial to have a good estimate of the velocity at all times. In the vehicles the transmission management system, TMS, where Opticruise is integrated, the velocity signal is obtained from other control units such as ABS and EBS systems. At Scania there has been a preference for modular solutions, thus there is a need for an alternative velocity signal that originates from within the TMS, based solely on the internal signals.[1]

The TMS control unit is currently equipped with a 2-axis accelerometer sensor, one in x-axis and one in the y-axis. The GPS is currently not on the TMS-controller but can be accessed through the internal, CAN-network. But with minor modifications, the control-unit could access this signal directly. To evaluate this sensor-

## CHAPTER 1. INTRODUCTION AND BACKGROUND

configuration, a more complete sensor model will be compared to a reduced, to see which sensors are the most important. The sensor set-up will be a central concept because there is an obvious incitement both economically and computational to have a minimal sensor set up, and the trade-off in loss of redundancy and robustness has to be investigated.

In applications like this project, low cost sensors will be used, and therefore it is crucial to fuse two or more sensors together such that they complement each other and reduce the overall error. But scenarios where temporary blackouts of some sensor, for example when GPS signal is lost in a tunnel, the system has to be robust enough to still provide a good estimate.

The Inertial measurement unit IMU consists of accelerometers that measures accelerations, and rate gyroscopes that measure angular-velocities. IMU's usually have very high updating frequencies and can detect small changes in forces and angles. But errors in the IMU will create drift in the lower order states when integrated. The main errors associated with inertial-sensors are noise and gravitational effects. Some of these errors can be limited by aligning sensors, and compensating for gravity. But for practical reasons this is not always achievable, because unobservability of these errors, especially in reduced sensor-configurations.

The GPS on the other hand will be unbiased, but the update frequency will be considerably lower than the IMU. So the GPS will detect the drift created by the IMU. The GPS signal will provide an velocity output in three-dimensions. From these velocities one can obtain the heading and velocity of the vehicle, but also the pitch.

Apart from the GPS and IMU, the TMS has a signal that is called the Output-shaft. This signal measures the rotational-velocity of the Output-shaft, and connects the wheels with the transmission. Therefore if scaled properly this signal will provide an accurate estimation of the velocity. But the Output-shaft will have problems with slippage when the wheels are spinning, and thus greatly reducing the reliability of the signal.

### 1.3 Literature

A lot of work has recently been done in the area of fusion between low cost IMU and GPS for a ground vehicle [5],[8],[9]. The usual sensor-configuration is either a six- or nine-axis IMU together with a GPS. They all show that with only these sensors an accurate and unbiased estimations for a ground vehicles course, attitude and velocities can be obtained. But because the vehicle is restricted to the road, there will be some axis that are less important than others to determine the attitude and direction of the vehicle correctly. Thus removing computational complexity and cost, it is interesting to remove all the unnecessary sensors that doesn't impede the overall accuracy of the signal.

Another approach is to replace the otiose sensors with a pseudo-signal. In [9] the

### 1.3. LITERATURE

signals from the sensors that were not providing critical information, or remained unchanged through the entire experiment, was replaced. For example removing the z-accelerometer with a constant value of  $9.82\text{m/s}^2$ . Thus standard algorithms for the full-sensor setup could be implemented.

Inertial sensors are not perfect and will have many sources of errors. There are both deterministic errors like Bias, and nonlinearities where the error is integrated over time. There are also stochastic errors like noise and velocity random walk. The deterministic errors can be accurately minimized with proper calibration. But these calibrations can deteriorate over time, because of unforeseen effects like temperature changes and other issues[13]. Drift is one of the issues that is given most of the attention, that is when the sensors accuracy deteriorate over time due to integration of the errors previously stated. To correct the drift, other sensor that doesn't drift over time, like a GPS, can be used for correction. One somewhat novel method to limit the drift of the sensors are called non-holonomic constraints. This in when in land vehicle applications, the velocities such that the vehicle is constrained. For example the velocities orthogonal to the directional direction is constrained, i.e. the vehicle can't jump or slide sideways, it is limited to the road[8] [11].

To fuse the different sensors and estimate the system states, the normal approach is to use a Kalman filter. A good filter according to [4], should fulfill three criteria. Filter consistency, which gives a good indication of the real system. Navigation system design, the choice of sensors should encapsulate the information required to observe all the states of interest. Fault detection, the filters are able to detect faults that occur in the sensor, models or the techniques used to detect these faults. The Kalman filter, if implemented correctly, fulfills all these requirements. There are various Kalman filters for non-linear systems, extended Kalman filter, extended information filter, and unscented Kalman filter are some examples. These methods are reliable and standard practice in industry, and have been implemented with great success [5] [9] [8]. These methods are extensively explained and derived in [4] and [8], both in continuous and discrete time. The extended Kalman filter is by far the most common for non-linear systems. It is a first order filter, because it linearises nonlinear state equations around the observed point using the Jacobian. In most cases the extended Kalman filter provides a good estimate, but unlike linear Kalman filter it is sub-optimal due to linearisation [2]. Another drawback with the extended Kalman filter is that it can be computational hard to solve, because the need to solve the Riccati equation, which can be demanding for large systems.

A relatively new method called Sliding mode observer. It is based on the same principles as the Sliding mode control. Compared to the Kalman filter it has a set of advantages, it is much easier to implement and not as demanding when it comes to processing power [18]. This is important in real time implementation. It also shows improvements to both noise attenuation and model errors. The downside is that the Sliding mode observer could, if not implemented correctly, start to show

## CHAPTER 1. INTRODUCTION AND BACKGROUND

chattering effects due to the nonlinear properties of the switching function [18]. Most literature about Sliding mode observers are single input single output systems in continuous time. But they provide the foundation of the multiple-input multiple-output systems (MIMO), i.e [20] proof for stability for matched and unmatched uncertainties with a discrete time Sliding mode observer with double boundary layers on a second order system was provided. Instead of the standard signum-function, a saturation function is used to reduce chattering.

In [22] both a continuous and discrete MIMO Sliding mode for a linear system was constructed, it also shows the basis existences of discrete time Sliding mode. In the literature there aren't many real-time implementation of Sliding mode observers, especially in the MIMO case. The most related work to this project is explained [10], where a Sliding mode observer for a four-wheel independent drive land vehicle is constructed. They used a full-vehicle model provided a Sliding mode observer that was chatter-free. The Sliding mode observer was able to estimate the roll angle of the vehicle, then using this relationship to estimate the vehicle velocity that is not dependent of the tire-road friction coefficients or road angles.

In [19], an observer based adaptive Neuro-Sliding Mode control for MIMO nonlinear systems were developed. It provided a rigorous proof for convergence of both the states and the state estimation. They used neural networks to estimate the nonlinearities. This report illustrates the benefits in combining Neural networks and Sliding mode control and Sliding mode observer. Some of benefits of neural networks are that it can provide an alternative to conventional methods in estimating nonlinearities. Neural networks are able to learn, understand and adapt, through rather simple methods explain complex a very complex behavior and patterns that would otherwise be very hard or impossible with standard methods. In [12] they used neural networks in fusion of an IMU and GPS, but also for the navigation algorithm. Neural Networks offer an convenient way to form models, and extract the essential characteristics.

# Chapter 2

## Methods

### 2.1 Sensor setup

#### 2.1.1 Sensor architecture

In the current control system of the latest generations of heavy duty vehicles, the TMS has a 2-axis IMU integrated in the control unit. It consists of 2 accelerometers oriented in the vehicles forward direction and to the side of the vehicle, has the capacity to send data with an update frequency of 100 Hz. The raw data from the GPS-signal is received with 5 Hz, the data is then transmitted over the internal CAN network such that the TMS can receive it, but only with 1 Hz. In Figure 2.1 a simple schematics show how the signals are transferred through the network. Because the GPS have potential to provide a much higher update-frequency an external GPS-receiver identical with the GPS in the vehicle was programmed such that it could transfer data at a higher frequency. It was connected directly to the computer through a serial port, and was transferred through a virtual CAN into the logging software Vision. In Figure 2.1 the bottom part of the image, a simplified illustration of the sensor structure and how it is logged. The components used are displayed in Figure 2.2.

To investigate which gyros and accelerometers were necessary a nine-axis IMU was purchased. 3 accelerometers, 3 gyros, and 3 magnetometers. Data was only collected from the accelerometers and Gyro-scopes, because the magnetometers will give the direction globally to the magnetic poles and not necessary in determining the velocity of the vehicle. To interface the IMU such that it could be transmitted and stored over the CAN-network, a micro controller that was equipped with a CAN-controller, was borrowed from the Mechatronics department at KTH.

The virtual sensors (vSen) software currently used in the TMS to obtain an estimate of the vehicles speed is based on the wheel-encoder [1]. To compare this estimation to the estimation made by the proposed algorithms a very accurate reference-GPS was borrowed. This reference GPS was connected directly to the computer and

## CHAPTER 2. METHODS

logged in Vision. This can be seen in the lower part of Figure 2.2.

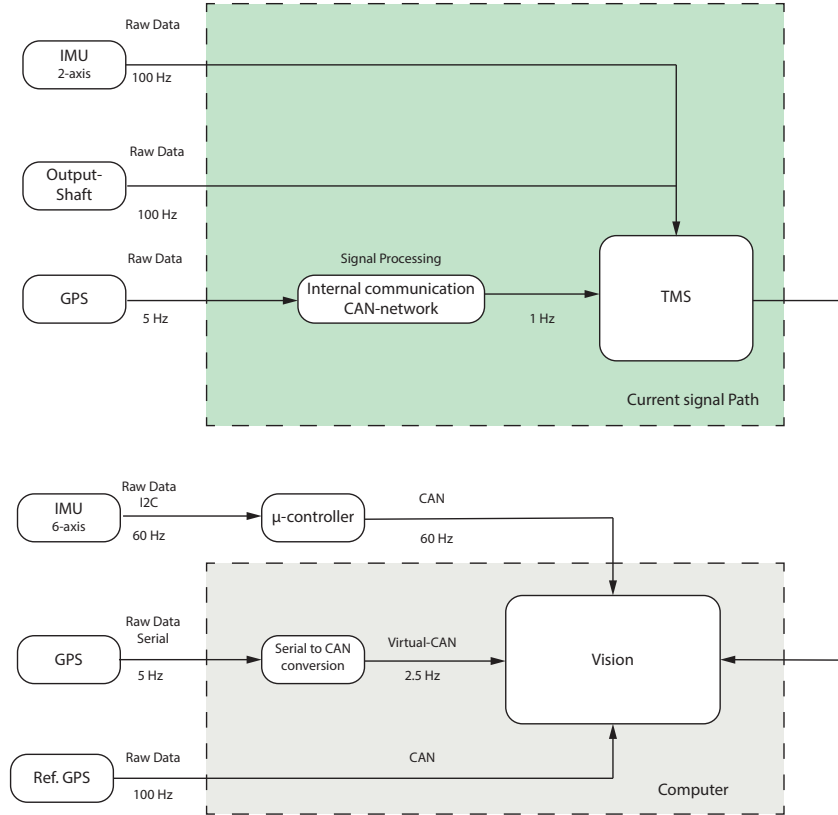


**Figure 2.1.** Image shows how the signals from the IMU, Output-shaft and GPS arrives in the TMS control-unit. In the bottom of the image shows how the sensors are interfaced and logged in vision.

## 2.1. SENSOR SETUP

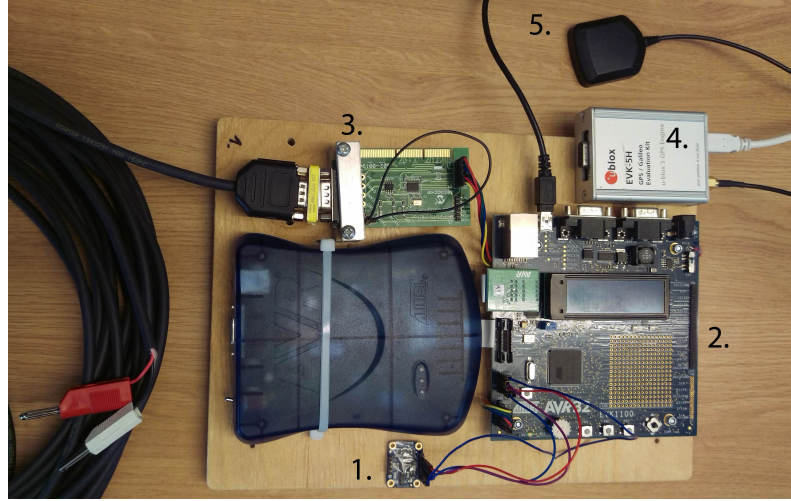


**Figure 2.2.** Image shows an image of the sensors. 1) is the 9-axis IMU, 2) the Atmel micro controller, 3) CAN-controller, 4) GPS-receiver 5) GPS-antenna

### 2.1.2 Sensor model & System equations

#### Accelerometer and Gyroscope

Cheap IMU's are far from perfect sensors, and will have errors associated with them. Errors associated with accelerometers are most commonly white noise. There are two different kinds of errors, stochastic and deterministic. Stochastic errors are white noise and random walks, and the deterministic errors are bias, misalignment, non-orthogonality, scale factor, and nonlinearities [14]. The following equations are obtained from [5], they represent the different acceleration contributions detected by the accelerometers:

$$a_x = \ddot{x} + 2V_y\omega_z + b_x + g \sin(\theta) + w_{acc}^x \quad (2.1)$$

$$a_y = \ddot{y} + 2V_x\omega_z + b_y + g \sin(\phi) + w_{acc}^y \quad (2.2)$$

$$a_z = \ddot{z} + g \cos(\theta) + b_z + w_{acc}^z \quad (2.3)$$

Where  $a_{x,y,z}$  are the measured acceleration,  $\ddot{x}$ ,  $\ddot{y}$  and  $\ddot{z}$  is the true acceleration in the vehicles coordinate system,  $b_{x,y,z}$  is the bias of the sensors,  $w_{acc}^{x,y,z}$  is white noise and  $\omega_z$  is the yaw-rate. For future reference  $\omega_y$  is the roll-rate,  $\omega_x$  is the pitch rate. The only deterministic errors considered will be bias and misalignment. Misalignment will be treated separately in another chapter. The stochastic errors will only consist of white noise. The gravity component in equation (2.2) will be neglected because a ground vehicle is normally not subjected to roll. Therefore most important gravity component will be the one linked to the pitch  $\theta$ . See Figure 2.3.

The Coriolis-force, note the terms in Equation (2.1) and Equation (2.2), i.e.  $2V_y\omega_z$ ,

will be restricted. In land vehicle application, some rotations and velocities are less likely to occur. Velocities like  $V_{z,y}$  are restricted because the vehicle doesn't slip or jump. But because the position of the IMU and GPS receiver would be located in the centre of rotation. This is not the case, therefore this will be a source of error due to the Coriolis effect. This error will only give a large error when the vehicle is turning rapidly. This phenomenon will be discussed in later sections.

The gyro is not affected by gravity in the same way as the accelerometers, it will be modelled to have a bias and noise. The following gyro-model is also obtained from [5].

$$g_{x,y,z} = \omega_{x,y,z}^{true} + b_r + v_{gyro} \quad (2.4)$$

Where  $g_{x,y,z}$  is the measured angular-rate  $\omega_{x,y,z}$  is the true angular-rate, and  $b_r$  is the bias, and  $v_{gyro}$  is zero mean white noise.

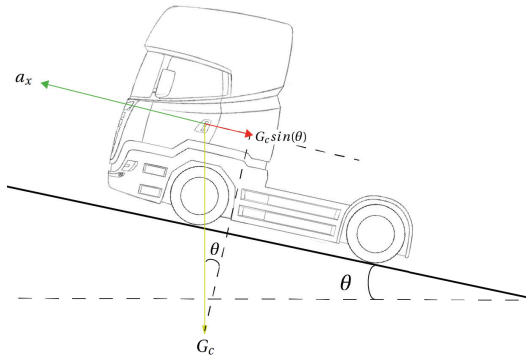


**Figure 2.3.** Image shows how the measurement is affected by gravity.

## 2.1. SENSOR SETUP

### Global Positioning System

The GPS can provide velocity measurements in three dimensions, either in the earth-frame or the inertial frame. See Figure 2.4. It is very common that a GPS can send both depending on preference. In this project the velocity measurements were sent in the earth frame. It is centered in the vehicle, and will provide the velocity coordinates north-east-down (NED). These measurements can then be used to obtain further information, such as the vehicles velocity, course, climb-rate and pitch. The following equations for pitch and velocity based on the GPS are obtained from [5].

$$V_{GPS} = \sqrt{V_{north}^2 + V_{east}^2 + V_{down}^2} \quad (2.5)$$

$$\theta_{GPS} = \sin^{-1}\left(\frac{V_{down}}{V_{GPS}}\right) \quad (2.6)$$

Where Equation (2.5) is the velocity of the vehicle, and Equation (2.6) is the Pitch.

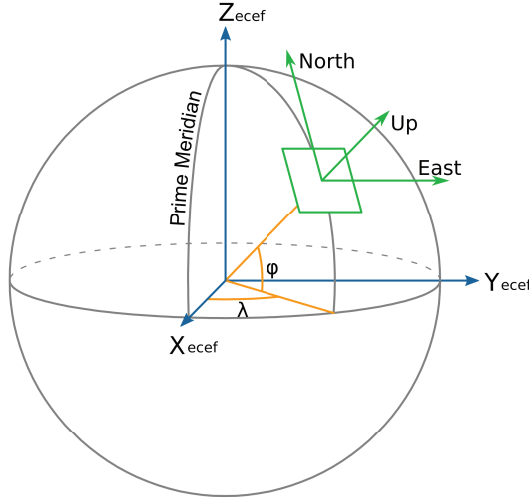


**Figure 2.4.** Earth centred frame, and navigation frame (NED). The GPS sends its measurements in the (NED) frame, green colors.

Equation (2.6) when  $V_{GPS}$  is small or zero, the arc-sinus function is either infinite or not defined. Resulting in a very inaccurate Pitch measurement. Thus the measurement will only be available after certain velocities. To illustrate this, the errors magnitude as a function of the vehicles velocity is showed in Figure 2.5. Indicating that the standard deviation tends to infinity when the velocity approaches zero. [5]

$$\sigma_{\theta_{GPS}} = \frac{\sigma_{GPS_{down}}}{V_{GPS}} \quad (2.7)$$

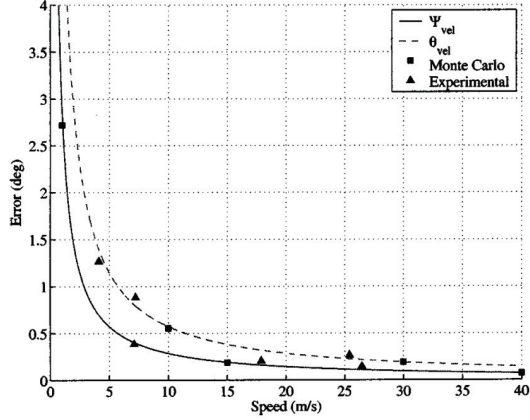


**Figure 2.5.** Illustrates the accuracy of the angles and how it changes with respect to the velocity. Image taken from [5]

### Drive-line and output-shaft

The drive-line is a fundamental aspect of obtaining a good vehicular model. There are several ways to model a drive, and they vary with respect to their intended use. In Figure 2.6 there is a very basic model of drive-line with the most important components. Because the TMS is the control-unit for the transmission, there is a direct measurement of the Output-shaft. The Output-shaft is connected to the propeller-shaft and because no friction between them is considered, it can be assumed that the Output-shaft is equivalent to the propeller-shaft. The final drive is characterized by a conversion ratio which equal is to a gear-ratio in the transmission[24]. Because a very simple model assuming the drive-shaft and the wheels are a lumped-mass, together with the assumption that the two wheels rotate with an identical speed. The equation for how the Output-shaft relates to the velocity can be simplified to a single constant, see Equation (2.8). This holds true when the wheels have no slip.

$$V_x^{shaft}(k) = C s_{shaft}(k) \quad (2.8)$$

## 2.1. SENSOR SETUP

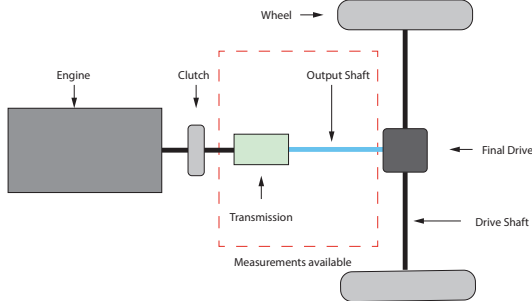


**Figure 2.6.** Depicts a simple drive-line model, and how the measurement of the Output-shaft relates to the velocity. Model and structure obtained from [24].

### 2.1.3 Unaligned sensors

If the IMU is considered isolated from other sensors, the different axis won't necessarily be perfectly aligned with the vehicles coordinate system. See Figure 2.7 This is very important in ground vehicle applications. This is because gravity is relatively large compared to the accelerations, produced by the motor. So an unaligned sensor will have large deviations from the true values due to gravity. To compensate this, the measurements needs to be transformed such that the measurements are aligned with the vehicle-frame. There are different methods to obtain rotation-matrices, the most common is refered to as the Direct cosine matrix (DCM). Which uses either euler-angles or quaternions to obtain a rotation-matrix, such that a measurement vector can be rotated between different coordinate-systems [4]. In the literature these methods are usually used to transform between different coordinate systems like the Earth frame, located in the earth center of mass and rotation and transforming it to the navigation frame. Which is the coordinate system where the vehicle has a coordinate towards north, east and down. This is an important transformation in GPS applications.

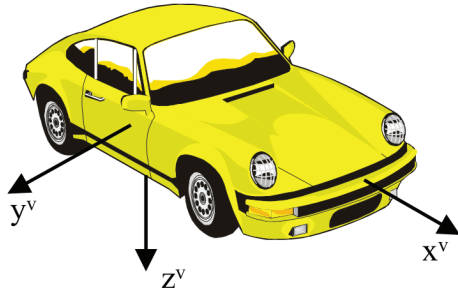


**Figure 2.7.** Image shows the vehicle centred frame.

But because the GPS-unit already transmits the velocity measurements in the NED

## CHAPTER 2. METHODS

coordinate-system, it is not necessary to preform this transformation in this project. But the same equations can be used simply to rotate a vector to another arbitrary coordinate system.

The use of Euler angles have downsides, the most problematic is that there will be singularities when the inverse-sinus function is performed. A better method is to calculate the direct cosine matrix using quaternions. It uses hyper complex variables to calculate the rotation of a vector along another vector in three dimensions [15],

$$\cos(\theta) = \bar{v}_1 \cdot \bar{v}_2 \quad (2.9)$$

$$\bar{w} = \bar{v}_1 \times \bar{v}_2 = \begin{bmatrix} w_1 & w_2 & w_3 \end{bmatrix} \quad (2.10)$$

$$\begin{aligned} \bar{q} &= \left[ \cos\left(\frac{\theta}{2}\right) \quad \sin\left(\frac{\theta}{2}\right)w_1 \quad \sin\left(\frac{\theta}{2}\right)w_2 \quad \sin\left(\frac{\theta}{2}\right)w_3 \right] = \\ &= \begin{bmatrix} q_1 & q_2 & q_3 & q_4 \end{bmatrix}. \end{aligned} \quad (2.11)$$

The first vector,  $v_1$ , would be the current IMU-measurement. The second vector,  $v_2$ , is the vector the first one is rotated to, usually the direction of gravity. The third vector  $w$  is the vector in which  $v_1$  is rotated around with the angle  $\theta$ . If the quaternion is normalized, the following rotational matrix can be constructed

$$R = \begin{bmatrix} (q_1^2 + q_2^2 - q_3^2 - q_4^2) & 2(q_2q_3 - q_1q_4) & 2(q_2q_4 + q_1q_3) \\ 2(q_2q_3 + q_1q_4) & (q_1^2 - q_2^2 + q_3^2 - q_4^2) & 2(q_3q_4 - q_1q_2) \\ 2(q_2q_4 - q_1q_3) & 2(q_3q_4 + q_1q_2) & (q_1^2 + q_2^2 - q_3^2 - q_4^2) \end{bmatrix}. \quad (2.12)$$

Because of the IMU is strapped down, it will be fixed in the vehicle frame and very unlikely that the orientation of the IMU will change relative the vehicle frame. It is a feasible assumption that the rotation matrix in Equation (2.12), will be constant. Thus this alignment step only need to be performed once on a flat surface, then saved for future use.

$$a_{x,y,z} = Ra_{x,y,z}^{Raw}, \quad (2.13)$$

$$\omega_{x,y,z} = R\omega_{x,y,z}^{Raw}. \quad (2.14)$$

## 2.2 STATE EQUATIONS

### 2.2 State equations

The state equations should capture the most important dynamics of the vehicle. Because there is no knowledge of the input to the system, like the demand of torque provided by the driver. The state equations are only dependent on the dynamics of the acceleration. The most important states are the pitch and the velocity. Thus there needs to be a state for both of them. Because the GPS will always be part of the sensor configuration, both the velocity and the pitch will be observable. The gyro will be considered if it will improve the estimation or not. Thus there needs to be two different state equations. State equations considering a gyroscope,

$$\hat{x}(k+1) = \begin{bmatrix} \hat{v}(k+1) \\ \hat{a}(k+1) \\ \hat{b}_v(k+1) \\ \hat{\theta}(k+1) \\ \hat{\omega}(k+1) \end{bmatrix} = \begin{bmatrix} \hat{v}(k) + \{\hat{a}(k) - g \sin(\hat{\theta}(k))\}\Delta t - \hat{b}_v(k) \\ \hat{a}(k) \\ \hat{b}_v(k) \\ \hat{\theta}(k) + \hat{\omega}(k)\Delta t \\ \hat{\omega}(k) \end{bmatrix} \quad (2.15)$$

$$\hat{y}(k) = h(x) = \begin{bmatrix} \hat{v}(k) \\ \hat{a}(k) \\ \hat{\theta}(k) \\ \hat{\omega}(k) \end{bmatrix} = \begin{bmatrix} 1 & 0 & 0 & 0 & 0 \\ 0 & 1 & 0 & 0 & 0 \\ 0 & 0 & 0 & 1 & 0 \\ 0 & 0 & 0 & 0 & 1 \end{bmatrix} \hat{x}(k) = H\hat{x}(k). \quad (2.16)$$

State equations that is not considering a gyroscope,

$$\hat{x}(k+1) = \begin{bmatrix} \hat{v}(k+1) \\ \hat{a}(k+1) \\ \hat{b}_v(k+1) \\ \hat{\theta}(k+1) \end{bmatrix} = \begin{bmatrix} \hat{v}(k) + \{\hat{a}(k) - g \sin(\hat{\theta}(k))\}\Delta t - \hat{b}_v(k) \\ \hat{a}(k) \\ \hat{b}_v(k) \\ \hat{\theta}(k) \end{bmatrix} \quad (2.17)$$

$$\hat{y}(k) = h(x) = \begin{bmatrix} 1 & 0 & 0 & 0 \\ 0 & 1 & 0 & 0 \\ 0 & 0 & 0 & 1 \end{bmatrix} \hat{x}(k) = H\hat{x}(k). \quad (2.18)$$

When there is a loss of a sensor like the GPS signal. The  $H$  matrix will be reduced such that only the accelerometer is available. This is done by setting the ones in the rows of the  $h(x)$  function representing the velocity and road grage to zero. [25]

### 2.3 Kalman filter

The Kalman Filter is one of the most common state estimation filters. The linear Kalman filter relies on linear state equation, it is also known as an optimal filter. It will be optimal if there is perfect information about the covariances of the system [2]. But in all real systems there are some nonlinearities, thus the need for an Extended Kalman-filter. It is generally good for sensor fusion application, and there

are a lot of literature of implementation of this filter. The following system is based on [6][7],

$$x_{k+1} = f_k(x_k) + w_k \quad (2.19)$$

$$y_k = h_k(x_k) + v_k \quad (2.20)$$

where  $x_{k+1}$  is the discrete state vector,  $y_k$  the output,  $w_k$  is the noise in the plant, and  $v_k$  is noise in the observation. Both are white Gaussian noise, with zero mean, and have the corresponding covariance matrices,

$$\text{cov} [v_k v_k^t] = R_k \quad (2.21)$$

$$\text{cov} [w_k e_k^t] = Q_k. \quad (2.22)$$

$Q$  is the covariance matrix associated with the model and the input noise, and  $R$  the covariance matrix of the measurement noise. The extended Kalman filter, is a first order filter. It linearise around the previous point to obtain an estimate about the next one. The higher order dynamics are assumed to be zero. Note the extended Kalman filter is not optimal like its linear equivalent, due to linearisation. The extended Kalman filter can be separated into two phases, the prediction step and the correction step. The prediction and correction is done recursively.

## Prediction

Here the  $P$  is the error covariance matrix,

$$P_{k|k} = \text{cov} [x_k - \hat{x}_{k|k}] \quad (2.23)$$

$$\hat{x}_{k+1|k} = f_k(\hat{x}_{k|k}) \quad (2.24)$$

$$P_{k+1|k} = F_k P_{k|k} F_k^T + Q_k. \quad (2.25)$$

Where  $F_k$ , and  $H_{k+1}$  are the Jacobian of the state equation and the observation.

$$F(k) = \frac{\partial f_k}{\partial x} |_{\hat{x}_{k|k}} \quad (2.26)$$

$$H_{k+1} = \frac{\partial h}{\partial x} |_{\hat{x}_{k+1|k}} \quad (2.27)$$

## 2.4. SLIDING MODE OBSERVER

### Correction

$K$  is the Kalman gain matrix.

$$K_{k+1} = P_{k+1|k} H_{k+1}^T \left[ H_{k+1} P_{k+1|k} H_{k+1}^T + R_{k+1} \right]^{-1} \quad (2.28)$$

$$\hat{x}_{k+1|k+1} = \hat{x}_{k+1|k} + K_{k+1} \left[ y_{k+1} - h_{k+1} \hat{x}_{k+1|k} \right] \quad (2.29)$$

$$P_{k+1|k+1} = \left[ I - K_{k+1} H_{k+1} P_{k+1|k} \right] \quad (2.30)$$

The Prediction and Correction set is repeated indefinitely.

## 2.4 Sliding mode observer

### 2.4.1 Non-linear Sliding mode observer

The Sliding mode observer will have similar structure as the Kalman filter, it can be compared to the prediction and correction step. The main benefit of the SMO is that it doesn't require any information of the covariances of the input signals or errors. Thus very effective for non-linear systems that are sensitive to model-errors. Another big benefit of the SMO compared to the Kalman-filter, is that it doesn't need to re-compute the Kalman gain, Equation (2.29), or the error covariance matrix, Equation (2.30). The Kalman gain is especially hard to compute due to the inverse matrix operation, which is computationally demanding for large systems. The downside of the SMO is that if implemented poorly it will have non-linear chattering phenomenon. The SMO is based on Lyapunov theory and will guarantee asymptotically convergence, if one can find a Lyapunov function. The chattering phenomenon can be limited with a proper choice of the switching function [20]. Because in this project the state equations will be nonlinear, there is a need for a nonlinear filter. Core-ideas and assumptions are quite similar between the linear and the non-linear Sliding mode observer [19][22]. For the non-linear system.

$$x_{k+1} = f_k(x_k) + B_k u_k + w_k \quad (2.31)$$

$$y_k = h_k(x_k) + v_k. \quad (2.32)$$

The following assumptions need to be considered,

**Assumption 1** the system is Bounded Input, Bounded States (BIBS).

**Assumption 2** the disturbances in the system are upper bounded [22].

If these conditions are fulfilled the Sliding mode observer will take the form, [18].

$$\hat{x}_{k+1|k} = f_k(\hat{x}_{k-1}) \quad (2.33)$$

$$\tilde{y}_k = y_k - h(\hat{x}_{k-1}) \quad (2.34)$$

$$\hat{x}_{k+1|k+1} = \hat{x}_{k+1|k} + K_{linear} \tilde{y}_k - K_{SMOSat}(\tilde{y}_k / \phi) \quad (2.35)$$

Where the gain is split into a linear feedback gain  $K_{linear}$ , and one switching gain  $K_{SMO}$ . To avoid the chattering phenomenon, that is usually a problem with the classical Sliding mode observer, the switching sigmoid function can be replaced with a saturation function.

$$sat(\tilde{y}_k, \phi) \equiv \begin{cases} \tilde{y}_k/\phi, & |\tilde{y}_k| \leq \phi \\ \text{sign}(\tilde{y}_k) & |\tilde{y}_k| > \phi \end{cases} \quad (2.36)$$

Where  $\phi$  is the width of the boundary layer. From [22] stability is proven with Lyapunov theory, and a lower and upper bound of the Sliding mode gain is provided. But like [18] an averaged Kalman gain for  $K_{linear}$  for fast tuning will be implemented.

## 2.5 Fusing two redundant signals

The Output-shaft and the GPS will make two independent observations of the velocity, and the true velocity is unknown. Therefore these two redundant measurement needs to be fused together. One method to fuse two redundant signals is the weighted least square (WLS). It utilises the knowledge of the individual sensors covariance and makes a weighted estimate[3].

$$\hat{x}_1 = x + \tilde{x}_1, \quad \text{cov}(\tilde{x}_1) = P_1 \quad (2.37)$$

$$\hat{x}_2 = x + \tilde{x}_2, \quad \text{cov}(\tilde{x}_2) = P_2 \quad (2.38)$$

$$P = (P_1^{-1} + P_2^{-1})^{-1} \quad (2.39)$$

$$\hat{x} = P(P_1^{-1}\hat{x}_1 + P_2^{-1}\hat{x}_2) \quad (2.40)$$

## 2.6 Testing, and Critical scenarios

To investigate the robustness of the proposed algorithms, data was collected from critical scenarios. At Scania Södertälje, there is a big test circuit that is constructed such that it replicates different scenarios a heavy-duty vehicle might encounter. A large variety of test-vehicles with different characteristics and performance are available for testing. The test were performed on a vehicle with normal specifications, and flexibility to place the sensor such that it could be easily mounted. Because the large variability of circuit, the test-scenarios could be decided beforehand.

### Hills

Hills are a critical scenario because the accelerometer is gravity-dependent as discussed in Section 2.1.2. If the pitch is omitted the error occurring in the accelerometer will make the velocity drift away from the true velocity in a small time period.

## 2.6. TESTING, AND CRITICAL SCENARIOS

On Scania's test-circuit there are several hills, with inclinations up to a road grade of 16%, or about  $9^\circ$ . Thus scenarios with both hills with large and small inclinations will be evaluated.

### Velocity extremes: Low- and High-speeds

Consider Figure 2.8, as indicated in the lower plot the wheel sensors will have an absolute error at high velocities. This is a scale-factor error, mostly due to an error in the estimation of the wheel's radius. Thus this is a clear area of improvement.

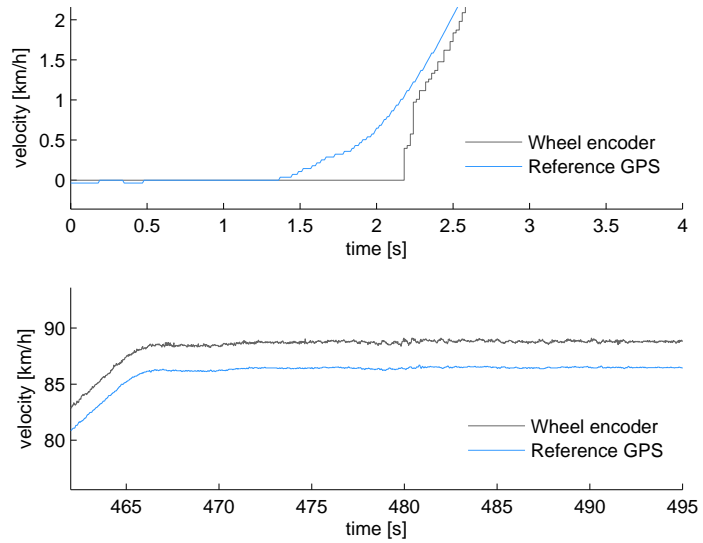


**Figure 2.8.** Illustrates where the velocity from TMS based on the wheel encoders have poor accuracy. At low velocities the wheel-encoders will not provide a signal before  $\approx 1m/s$ , showed in the top image. Due to a scale-factor error the wheel encoders will also have poor properties at high velocities, illustrated in the lower image.

Also indicated in Figure 2.8 in the top plot, the current method have issues at the lower velocity spectrum as well i.e.  $\approx 0 - 1m/s$ . The wheel encoders will provide a velocity signal after a certain threshold. Thus this scenario is most desirable for Scania to improve.

### Signal deterioration: slip and GPS outage

Because both the GPS and the Output-shaft have problems with reliability, becoming lost or bad, for example when the Output-shaft will start to slip, or the GPS is lost due to driving inside a tunnel. Normally one signal can be complemented by the other. But this doesn't prevent the system from being bad all together, both

the GPS and Output-shaft are bad at the same time. Thus one critical scenario would be if the entire velocity signal is lost and then investigate how the system behaves.

## 2.7 Slip detection

The Output-shaft will give a accurate velocity signal if scaled properly. But because the Output-shaft provides torque to the driving wheels, when the tires loose friction and starts to spin the signals accuracy will decrease. Thus it is very important to have a good indication when the wheels start to spin. Because it was hard to simulate wheel slip on the test-track. Data of slip was obtained from tests conducted at Scanias yearly tests in winter conditions. To obtain the slip such that it could be added artificially to other data, the true velocity was compared to the velocity signal from the Output-shaft. The result is shown in Figure 2.9.

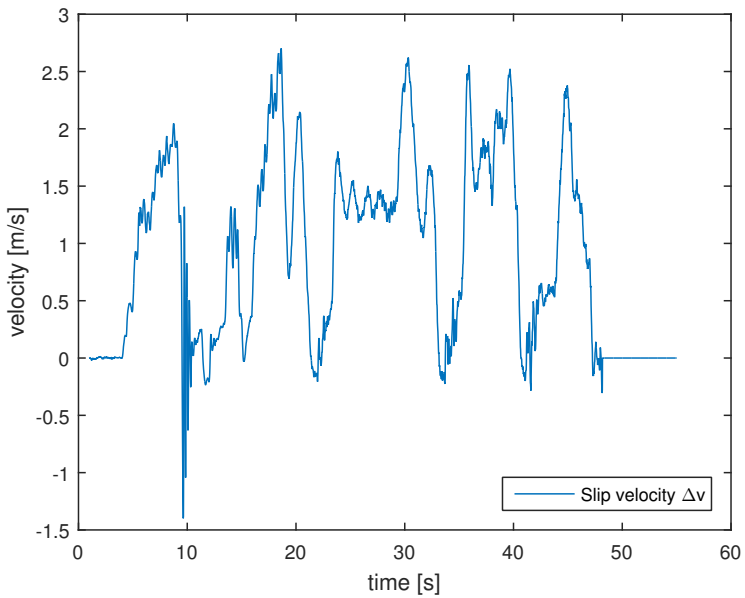


**Figure 2.9.** Image of the velocity difference between the actual velocity and the velocity measured by the Output-shaft. Obtained from a winter-scenario where a vehicle slips due to poor friction.

To obtain a good indication when the Output-shaft was slipping, it is usually a good idea to look at the signals derivatives. It will reveal high frequency changes like oscillations. But derivatives of an already noisy signal is also noisy. Thus is not suitable to quantify an answer whether the signal is good or not. One solution might be to investigate the energy of the signal. Because most signals don't have finite energy it is interesting to look at a signals energy during finite time [2]. This also saves a lot of computational effort saving data from a short period prior. This

## 2.8. LATENCY COMPENSATION

might reveal some information of the slip in the signal. Thus one might look at the RMS during a short period of time.

$$RMS(\bar{x}) = \sqrt{\frac{1}{N}(x_1^2 + x_2^2 + \dots + x_n^2)} \quad (2.41)$$

But as Figure 2.9 indicates there are low frequency components in the slip, and the RMS will be good at detecting high frequency content. The variance of the signal was proven to be a better indicator.

$$Var(\bar{x}) = \frac{1}{N} \sum_{k=1}^N (x_k - \mu)^2 \quad (2.42)$$

Where  $\mu$  is the average.

To quantify when the Output-shaft is bad, different logical conditions will make a decision to trust the Output-shaft or not. The first flag will indicate if the Output-shaft is slipping and the second flag will indicate if there is a velocity difference between the GPS and Output-shaft, and the third flag will indicate if the vehicle is turning very rapidly. These three flags will realize which of the Output-shaft or the GPS is deviating from the true velocity.

## 2.8 Latency compensation

In real systems there will always be latency associated with the implementation. The GPS will have more latency compared to the Output-shaft or the accelerometer. This is because the signal needs to be processed and converted, and in the process creating latency. Because the computational effort will be somewhat constant, the delay will also be constant. Which simplifies the problem considerably. There are several ways to handle measurement delay. The easiest and the most inaccurate is to ignore that there are delay. This will be the most computational efficient. Another method is to re-calculate the entire time-trejectory. This will be very demanding both storagewise and computationally, and grows larger the longer the time delay[17].

The Latency compensation method with the Kalman filter is in accordance with the method described in [16], and is referred to as Larsens method in [17]. The principle is that you have two parallel filters, one that calculates the state estimation when the measurement arrives, as if there was no delay. The other filter starts at time  $l = k - N$ , where  $N$  is the number of samples the delay represent, and uses the covariance  $R_k^*$ . Up until the time  $k$ , the estimates from the first filter will be used. But when the delayed measurement arrives, the measurement will be fused in the parallel filter. The measurement vector is then extrapolated.

$$y_k^{int} = y_k^* + H_k^* \hat{x}_k - H_l^* \hat{x}_l \quad (2.43)$$

where  $l = k - N$  and  $N$  is the number of samples the delay represents.  $y_k^*$  is the non-delayed measurement. Through  $N$  succeeding time data updates from time  $l$  to  $k$ , the estimation error covariance therefore becomes:

$$M = E\{\tilde{x}_l \tilde{x}_k^T\} = P_s \prod_{i=0}^{N-1} A_{k-i-1}^T (I - K_{k-i} H_{k-i})^T \quad (2.44)$$

$$M_* = \prod_{i=0}^{N-1} (I - K_{k-i} H_{k-i}) A_{k-i-1} \quad (2.45)$$

The new updated Kalman gain.

$$K_k = M_* P_l H_l^{*T} [C_l^* P_l H_l^{*T} + R_k^*]^{-1} \quad (2.46)$$

Updating the covariance matrix of the error.

$$P_{k+1|k} = P_{k|k} - K_k H_l^* P_l M_*^T \quad (2.47)$$

Then if adding the following expression after  $y_k$  has been fused.

$$\delta \hat{x}_k = M_* K_l (y_k^* - H_l^* \hat{x}_l) \quad (2.48)$$

Adding this extra filter will naturally increase the computational load.

This idea can translate to the Sliding mode observer. Extrapolate the measurement using equation 2.43, then using the measurement update step equation 2.35 to obtain  $\hat{x}_l$  with the correct non-lagged measurement. The extrapolated measurement will then be fused in the in the filter normally. But this method is suboptimal[17].

# **Chapter 3**

## **Results**

### **3.1 General characteristics of the signals, and results**

#### **3.1.1 GPS**

As mentioned in Section 2.8, the GPS-measurement will be delayed. This is illustrated in Figure 3.1, where the GPS signal is shown together with the highly accurate reference GPS. The raw GPS-signal has a constant delay of  $500ms$ . If the signal is shifted  $0.5s$  backwards in time the GPS-signal will accurately follow the reference GPS. When comparing the raw GPS-signal with the original GPS signal with  $1Hz$  from the CAN-network, the GPS only has a delay of  $250ms$ . This is most likely due to suboptimal sensor-architecture and interfacing. This will be a future area of improvement. But if the interfacing was optimised, one might expect to reduce the delay at least to match the level that is currently in the TMS. Therefore it is justified to shift the signal such that there is only a delay of  $250$  ms in the GPS-measurement. This will make the comparison between the current wheel-encoder (WE) estimate and the proposed methods more comparable.

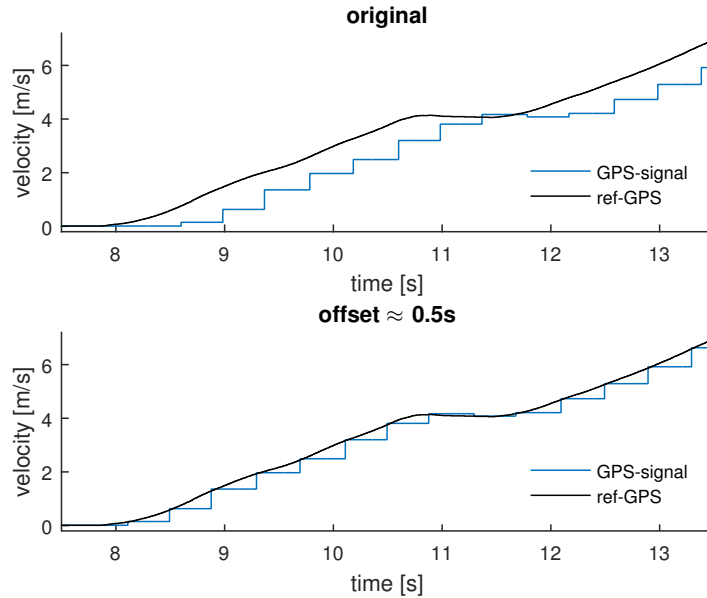


**Figure 3.1.** The top figure the raw GPS-signal is shown together with reference GPS. In the lower image the same signal is shifted 0.5 s in time. The shifted signal follows the reference accurately.

### 3.1.2 Alignment of strap-down IMU

In Section 2.1.3, a misalignment of the strap-down IMU was discussed together with a method to compensate for it. As shown in Figure 3.2 the misaligned IMU can be centred to the vehicle frame. This is done such that it is aligned along the direction of gravity. This requires that there is no accelerations other than gravity. This would require that the vehicle is on a flat surface when the algorithm is performed, otherwise the IMU will not be aligned properly. But because it is unlikely that the strap-down IMU change its orientation relative the vehicle frame, the rotation matrix will remain constant. Thus by saving a matrix from a scenario where the vehicle is on a flat surface, the matrix can be reused. The alignment step can be performed again to align the IMU in the xy-plane. This would require that there is a clear signal of an acceleration in the forward direction.

### 3.1. GENERAL CHARACTERISTICS OF THE SIGNALS, AND RESULTS

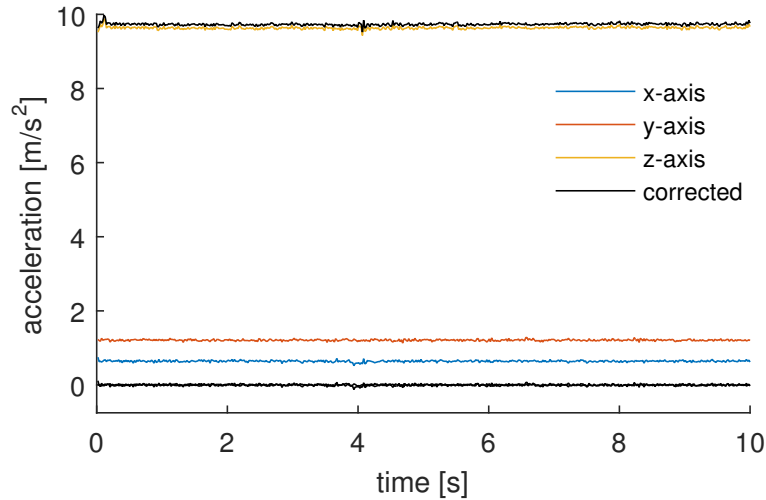


**Figure 3.2.** Illustrates how an miss-aligned accelerometer configuration is able to align the accelerometers to the vehicle frame.

#### 3.1.3 Output-shaft

The Output-shaft, if compared to the GPS, will not provide as accurate velocity estimation. As shown in Figure 3.3 the Output-shaft will be noisy and have oscillations, especially when the vehicle switches gear. As discussed in Section 2.7, the Output-shaft will slip in bad conditions. But unlike the GPS, the Output-shaft will never have outages and have a much higher update frequency.

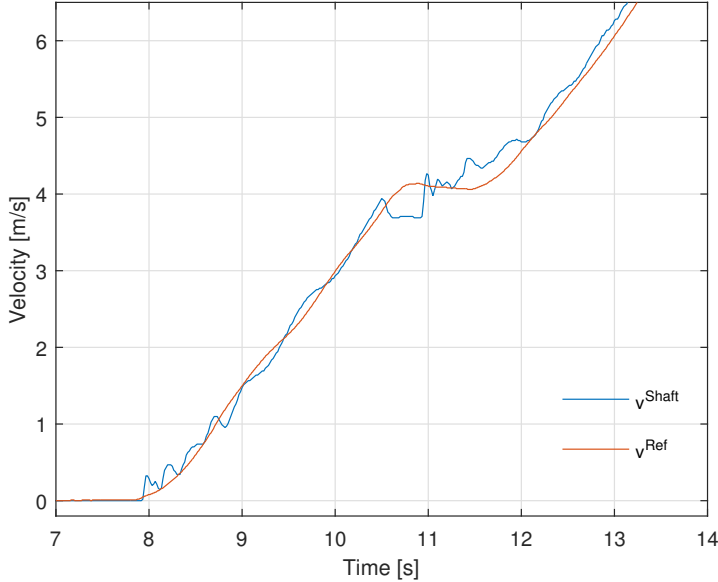


**Figure 3.3.** Image shows the typical Output-shaft signal, when scaled properly. In the image one can clearly see gear switching, time  $10.5[s]$ , which will make the signal oscillate.

### 3.2 Comparison Kalman vs. Sliding mode

In this section the difference between the Sliding mode observer (SMO), Extended Kalman filter (EKF), and the current TMS wheel encoder based velocity estimation from Scania is explored (TMSWEE). In the tables the root mean square error (RMSE), mean absolute error(MAE), and the peak error or the largest error occurring in this sequence are displayed. Two different scenarios was used to illustrate the differences. A small hill, making the pitch an important state to estimate. A longer scenario with high speeds, fast accelerations and to investigate the overall performance of the filters.

#### Small hill

In Figure 3.4 the result from the two different filters are displayed, and the resulting error-analysis is shown in Table 3.1. Both the EKF and the SMO have better performance than the TMSWEE in both the root-mean-square error (RMSE) and mean-absolute error (MAE). If one investigates the figure this is occurring when the vehicle is de-accelerates rapidly. Thus the large amplitude error is due to the fact that the GPS is delayed and the entire signal will have an offset.

### 3.2. COMPARISON KALMAN VS. SLIDING MODE

	<i>Kalman Filter</i>	<i>Sliding mode Observer</i>	<i>TMSWEE</i>
<i>RMSE</i>	0.5742	0.5652	0.7062
<i>MAE</i>	0.4571	0.4484	0.5996
<i>Peak Error</i>	1.5370	1.5178	1.4040

**Table 3.1.** Comparison of the Extended Kalman Filter, the Sliding mode observer, and the current method from the TMS based on wheel encoders (TMSWEE). This is from the scenario where the vehicle is driving up a small hill.

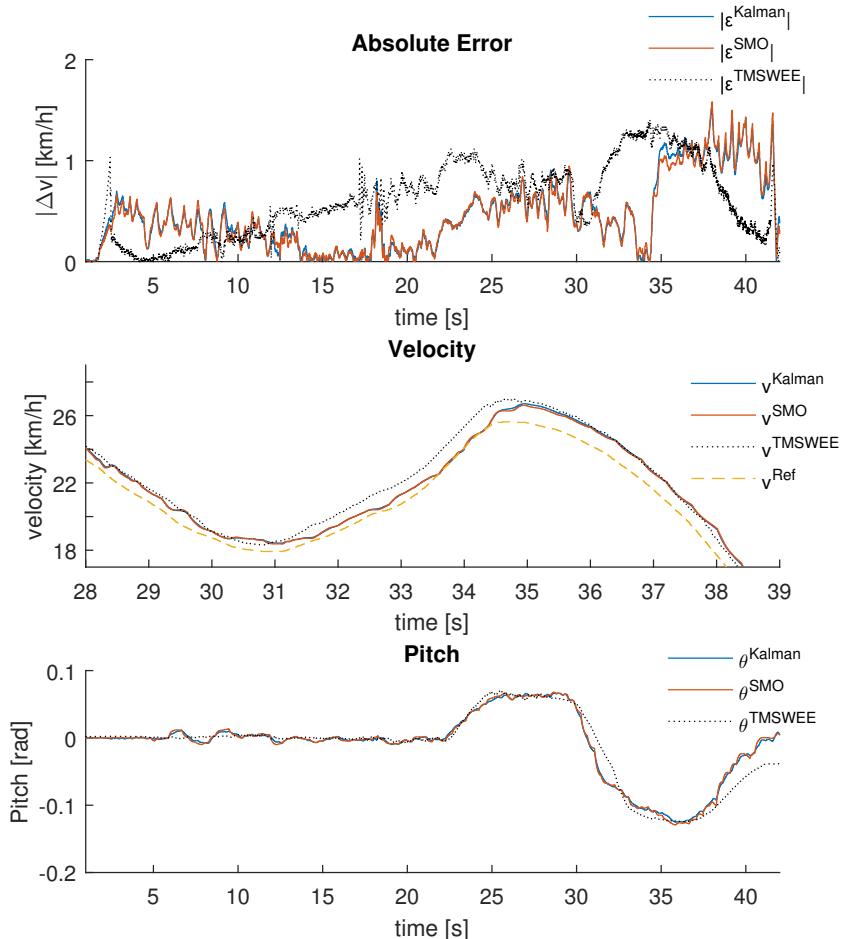


**Figure 3.4.** This picture shows a drive-scenario from a small hill. In the top image the absolute error in the estimated velocity compared to the reference GPS's "true velocity" is displayed. In the middle image displays the velocity-estimation from the SMO and Kalman, together with the reference GPS and the TMSWEE. The image is also zoomed in on the velocity when the vehicle is driving over the hill. In the bottom image the pitch is displayed.

### Long drive

In Figure 3.5 the error, velocity and pitch is displayed. In the bottom image the pitch is displayed. One can see that both the SMO and EKF has a large error in the pitch in the beginning. The reason for this error is the initial state of the pitch, and the filter takes some time before it converge to the real value.

The plot in the middle is velocity-estimation and the top plot the corresponding absolute error to the velocity estimation is displayed. In the beginning the velocity has this saw-tooth appearance, the tooth's are when the vehicle switches gears, this will cause the velocity to have a sharp deceleration. Because the GPS will have latency, and the Output-shaft will have large oscillation. This will translate into a large error-peak. The second important observation is that both filters will be better than WE during high speeds, because the GPS will be bias-less. But because the GPS signal and the Output-shaft is fused with weighted least square (WLS) the velocity measurement will inherit error in the scale factor, from the Output-shaft. But from this scenario the proposed filters will have better performance than the current TMSWEE, the error analysis is shown in Table 3.2.

### 3.2. COMPARISON KALMAN VS. SLIDING MODE

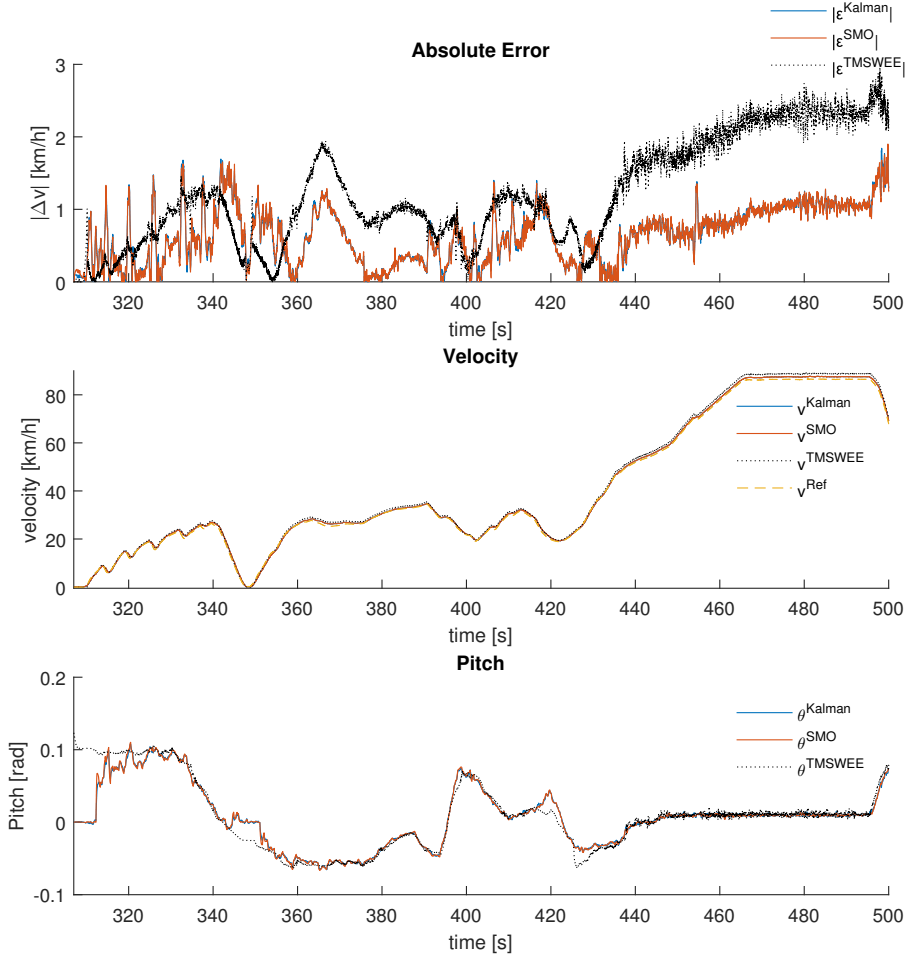


**Figure 3.5.** This image displays a longer driving-scenario when the vehicle is subjected to fast accelerations, and both low- and high-velocities. In the top image the absolute error in the estimated velocity compared to the reference GPS's "true velocity" is displayed. In the middle image displays the velocity-estimation from the SMO and Kalman, together with the reference GPS and the TMSWEE. In the bottom image the pitch is displayed.

	<i>Kalman Filter</i>	<i>Sliding mode Observer</i>	<i>TMSWEE</i>
<i>RMSE</i>	0.8509	0.8468	1.5822
<i>MAE</i>	0.7441	0.7416	1.3696
<i>Peak Error</i>	2.7772	2.7122	3.6360

**Table 3.2.** Comparison of the Extended Kalman Filter, the Sliding mode observer, and the current TMSWEE. This is from the case where the vehicle is a case where there is a longer drive with both hills, high- and low-velocities.

### 3.3 Improving the sensor configuration

To evaluate if there are any benefits in having a more complete sensor-configuration, a gyro was added to the state equation to provide an observation on the pitch's angular-velocity. This was then compared to the sensor-configuration that resembles what is currently available from the TMS. The reference-GPS bases its estimation on an IMU with very high quality and a GPS. These raw-signals are available. The accelerometers in from the IMU used in this project had relative good accuracy, but the gyroscope's was not. Therefore to investigate how a much better the estimate becomes with an accurate IMU, the gyroscope measurements from the reference-GPS will be used, then compared to the normal gyro.

Another area where a more complete sensor-configuration is beneficial is in the case when the vehicle is subjected to a sharp turn. Because the GPS-receiver will not be in the centre of rotation, the GPS will measure slip-velocity. That is the velocity around the centre of rotation. Because the vehicle is also turning the Coriolis effect, Equation 2.1, will make the x-axis accelerometer inaccurate. But because the Output-shaft does not measure this slip of the GPS, the velocity difference will be the slip velocity of the GPS. If one adds a yaw-gyroscope  $\omega_z$ , thus the Coriolis-acceleration is observable and its error on  $a_x$  can be compensated for.

#### Pitch-gyro

In Table 3.3 the two different models were evaluated when the Output-shaft was available. Both estimations are accurate considering difference in the RMSE and MAE between the two filters.

In the case where the Output-shaft is omitted, the need for a gyro becomes more apparent. This is displayed in Table 3.4. The filters were evaluated when the velocity and pitch measurement was limited to only the GPS-signal and IMU. Where the pitch have rapid changes, the gyro-less system will have inaccurate information of the pitch in between the GPS-samples due to the slow update-frequency of the GPS. Resulting in an inaccurate gravity compensation on the accelerometer. The velocity estimation will therefore have a peaky appearance between the GPS samples and then jump back when the GPS-signal arrives. This will make the overall RMSE and MAE increase, compared to the setup with a rate gyro.

### 3.3. IMPROVING THE SENSOR CONFIGURATION

	<i>Without Gyro</i>	<i>With gyro</i>	<i>TMSWEE</i>
<i>RMSE</i>	0.5762	0.5756	0.7062
<i>MAE</i>	0.4572	0.4580	0.5996
<i>Peak Error</i>	1.5721	1.5372	1.4040

**Table 3.3.** This table shows a summary of errors comparing the benefits of adding a rate-gyroscope and not having a rate-gyroscope, when the Output-shaft is available.

	<i>Without Gyro</i>	<i>With gyro</i>	<i>TMSWEE</i>
<i>RMSE</i>	0.6271	0.5115	0.7062
<i>MAE</i>	0.5078	0.4187	0.5996
<i>Peak Error</i>	1.7827	1.4219	1.4040

**Table 3.4.** This table shows a summary of errors comparing the benefits of adding a rate-gyroscope and not having a rate-gyroscope, when the Output-shaft is not available.

### A better Gyroscope

Here the scenario where the vehicle is driving in a small hill was considered. At a critical point in the scenario where the pitch will change rapidly, all the signals that provides a velocity estimation was removed such that the system had to rely solely on the IMU. In Figure 3.6, the resulting pitch estimation is illustrated. In the bottom figure the normal gyroscope is used. It will start to deviate rapidly after 5 seconds. The accurate IMU from the reference GPS will however have a much more accurate pitch estimation. In Figure 3.7 the corresponding velocity is shown. The estimation with the normal gyroscope will diverge rapidly compared to the estimation with the better gyroscope.

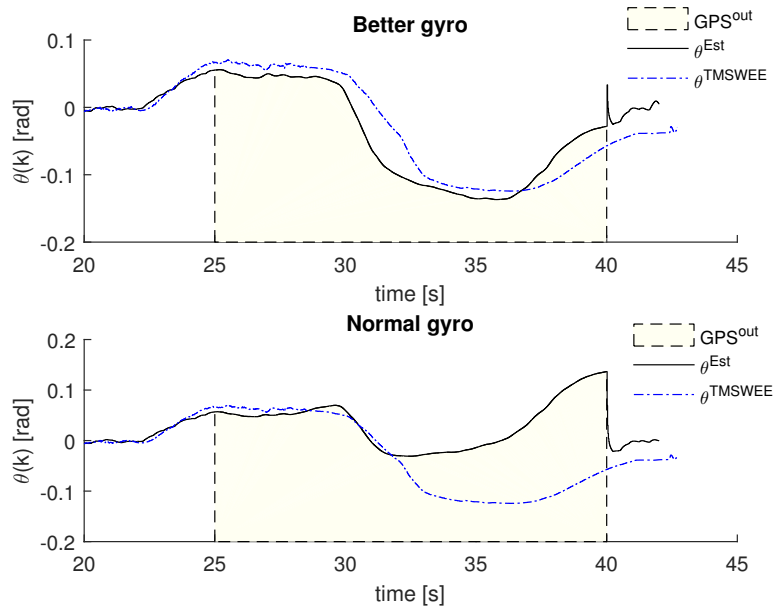


**Figure 3.6.** Image shows the improvement of the estimation of the pitch with a better gyroscope. During a simulated complete blackout of the velocity measurement, loosing both the GPS and Output-shaft signal.

### 3.3. IMPROVING THE SENSOR CONFIGURATION

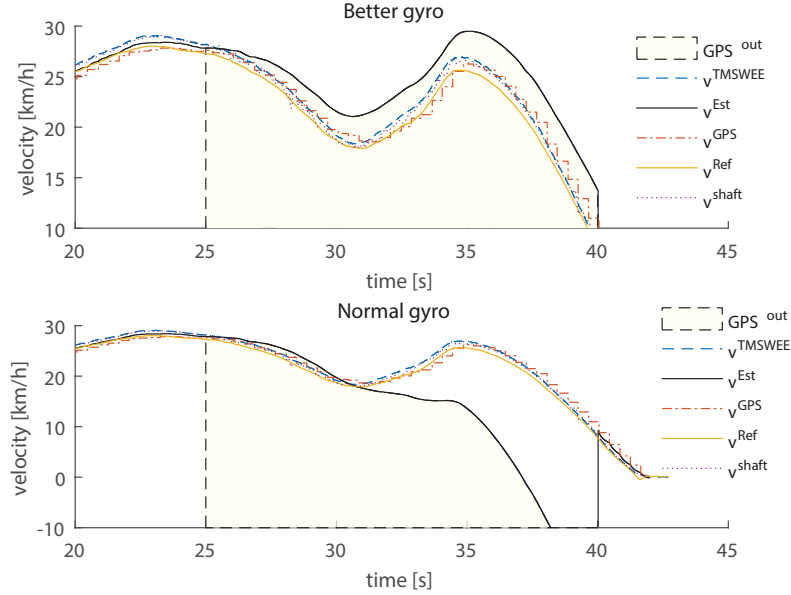


**Figure 3.7.** Image shows the improvement of the estimation of the velocity with a better gyroscope. During a simulated complete blackout of the velocity measurement, loosing both the GPS and Output-shaft signal.

#### 3.3.1 Coriolis

In Figure 3.8, the velocity measured by the GPS, from the scenario where the vehicle is turning rapidly on a flat surface. The Output-shaft is displayed in the bottom figure. There is a clear velocity difference at two time intervals 10 – 20s and 80 – 95s. Similar velocity differences are observed in the velocity from the TMSWEE. The reason for this is that the GPS is not located in the centre of rotation. So when the vehicle is turning the GPS is also measuring a velocity around the centre of rotation together with the true-velocity. The same goes for the velocity estimation from the TMSWEE, because the wheel encoders are located in the front-wheels. For clarification see A.2. In the top figure the y-axis accelerometers output is displayed together with the calculated Coriolis-effect,  $a_{Coriolis}$ . It was calculated by multiplying the velocity difference between the Output-shaft and the GPS-measurement, multiplied by the yaw angular-velocity,

$$a_{Coriolis} = (v_{GPS} - v_{Shaft})\omega_z. \quad (3.1)$$

The yaw angular-velocity displayed in the middle figure.

Because of this error in the velocity-measurement, it is desirable to omit the GPS-measurement during these instances where the Coriolis is present. Consider Section 2.7 where the slip detection algorithm was described. It is important to flag when the GPS is un-trustworthy and when the Output-shaft is slipping. Thus the Coriolis-effect would be the ultimate indicator for when the GPS needs to be ignored. But

### CHAPTER 3. RESULTS

one needs a minimum of 3 sensors to calculate the Coriolis: Output-shaft,GPS and gyro. The latter is not available in the current generation of TMS. Therefore an alternative method to detect slip-velocity is needed.

If the acceleration  $a_y$  is considered in isolation, it will contain the centrifugal acceleration, and the acceleration that is producing the slip-velocity. Because there is one known and there are two unknowns, it is impossible to extract either.

Consider the middle and top plot in Figure 3.8,  $\omega_z$  and  $a_y$  will have a very similar appearance. So if the acceleration in the y-direction is large and there is a velocity difference between the GPS and Output-shaft, the GPS is most likely subjected to slip. Thus for the purpose of indicating when there is slip, the y-acceleration can replace Coriolis.

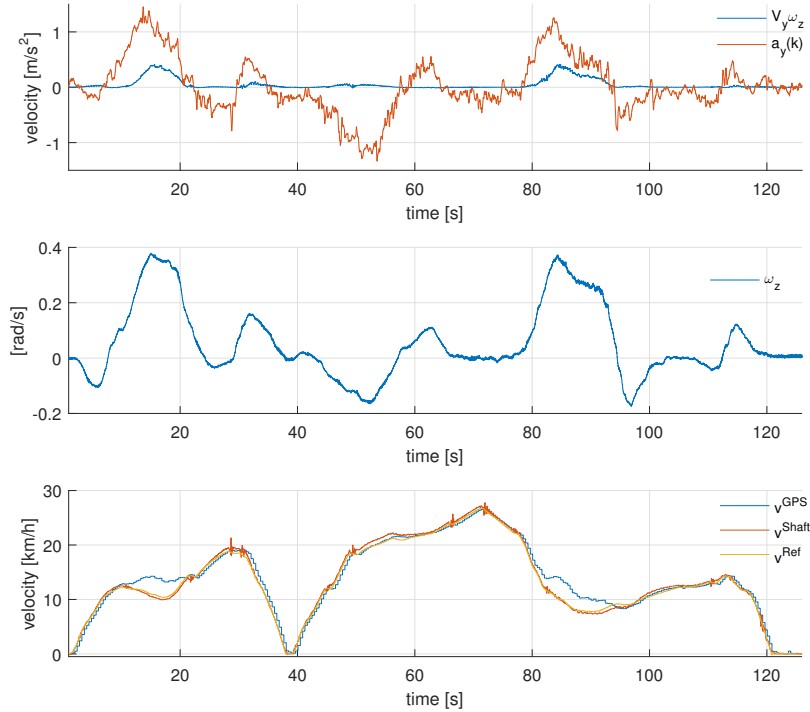


**Figure 3.8.** The top figure shows the Coriolis-effect compared to the measured acceleration on the y-axis. In the middle image the yaw-rate is displayed, and in the bottom image velocity from the Output-shaft and the GPS is compared. There is a large velocity difference during sharp turns.

To illustrate how much the Coriolis-effect will impact the velocity estimation, the top image in Figure 3.9 shows the calculated Coriolis-acceleration. In the middle image the accelerometer measurements are simply integrated to obtain the velocity, together with the true velocity. In the bottom image the acceleration measured is

### 3.3. IMPROVING THE SENSOR CONFIGURATION

displayed together with the Coriolis corrected acceleration.

If the Coriolis-acceleration is removed from  $a_x$  the velocity estimate will be closer to the true-velocity of the vehicle. As the image indicate the Coriolis corrected accelerometer will start to drift after about 40s compared to 5s from the uncompensated.

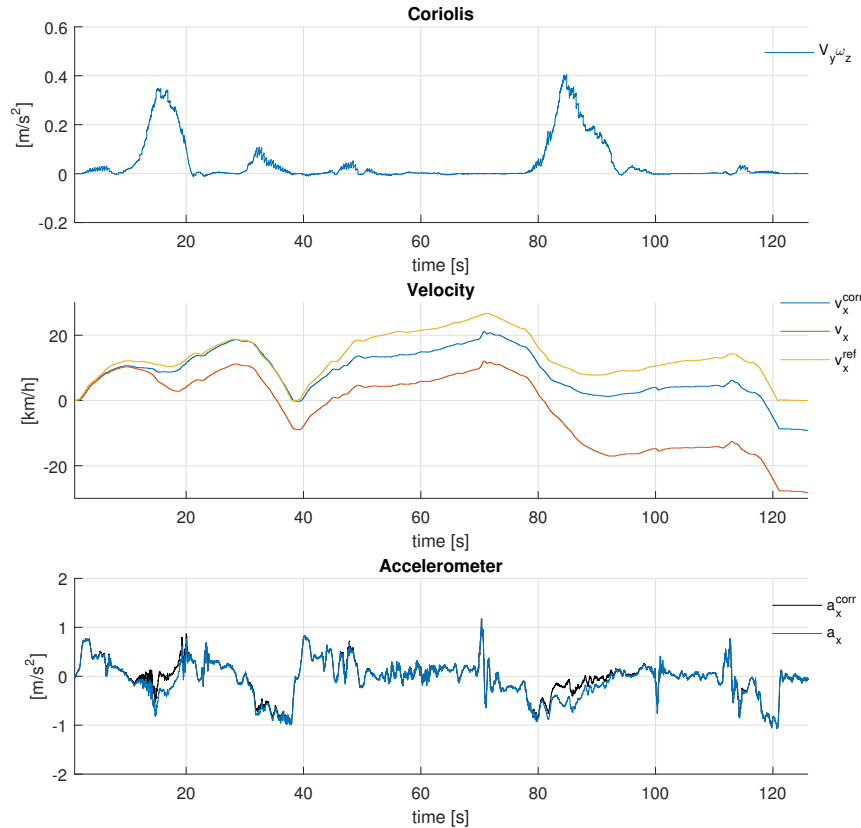


**Figure 3.9.** Image shows the benefits of compensating for Coriolis-accelerations for the measurements. In the top plot the Coriolis-acceleration in the x-direction is displayed. In the middle image the velocity from integrating the acceleration measurement, before and after compensating for Coriolis together with the true velocity is displayed. In the bottom plot the measurement of the acceleration is displayed before and after compensating for Coriolis.

## 3.4 Robustness

In this section the robustness of the estimations is considered. What would happen if a signal was lost or considered bad, for example the GPS is lost if there is a bad reception, in a tunnel or in a City with high buildings.

The Output-shaft will provide an accurate velocity estimation with high frequency, but the Output-shaft have some big issues in robustness. Especially in bad conditions, when the wheels loses grip. In Section 2.7 a method for detecting this slip was proposed.

Then the algorithm will be evaluated such that it preforms in both high and low velocities.

### 3.4.1 GPS-outage

Because Scania's test-circuit is outside, and no tunnels are available, the GPS-outage had to be added artificially. To simulate this behaviour, the GPS signal was considered as completely lost with no transition phase of deteriorating accuracy, like going into a tunnel. Two sensor-configurations are interesting to evaluate during a GPS-outage: with and without an Output-shaft signal.

If there is no Output-shaft observation the system needs to rely solely on the IMU to provide a estimate. As discussed in Section 3.3, it is important to have accurate IMU-sensors to maintain an accurate estimation during this outage period. Otherwise the system will have similar behaviour to Figure 3.7, and diverge from the true velocity rapidly.

If there is an observation of the Output-shaft and the GPS, the system will be more reliable. The system will be vulnerable to errors in the Output-shaft observation, but it will be better than the previous scenario. The result of a GPS-outage with observation of the Output-shaft is displayed in Figure 3.10. In the top of the figure the absolute error is displayed. The proposed method without the GPS will out perform TMSWEE during the period of the outage. The corresponding velocity profile is displayed in the image below.

### 3.4. ROBUSTNESS

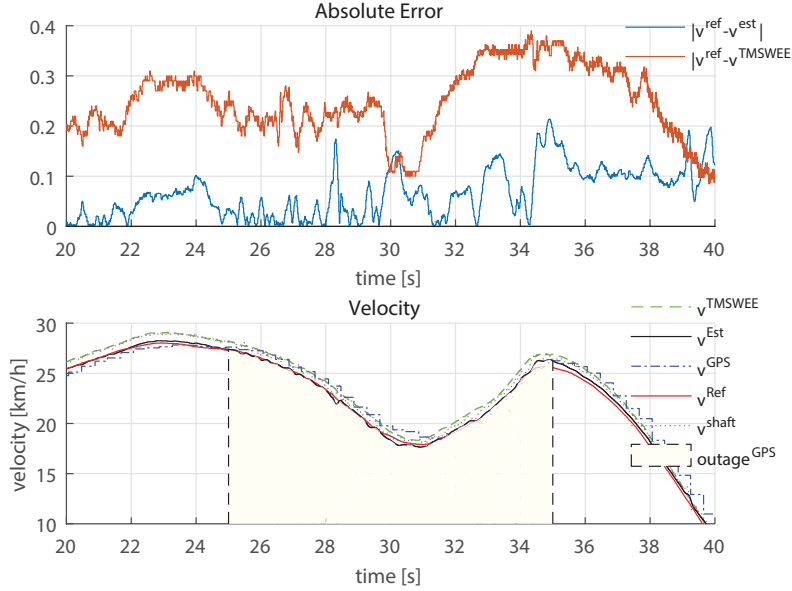


**Figure 3.10.** Illustrates the velocity estimation when the GPS has an outage. Because the Output-shaft is still available the signal remains more accurate than TM-SWEE. But when compared to the fused GPS and Output-shaft, the estimation becomes slightly more noisy.

#### 3.4.2 Slip Detection

In Figure 3.11 the signals used to indicate slip in both the Output-shaft and GPS is showed. The thresholds are indicated with a straight line, and black lines are indicating when the algorithm flags for a possible slip-scenario. Three different flags were constructed to quantify when a signal might be bad.

- Flag 1: There is a velocity difference between the GPS and Output-shaft.
- Flag 2: The variance in the Output-shaft during the last  $N$  samples is high.
- Flag 3: The magnitude of the acceleration in the y-direction is high.

The bottom image shows the decision made by the algorithm, where the different levels illustrates the actual decision. There are 3 different decisions:

- All sensors are good
- Trust IMU and GPS, Flag 1 and Flag 2 is active.
- Trust IMU and Output-shaft, Flag 1 and Flag 3 is active.

The sharp turning driving-scenario was chosen, because it has areas where the GPS will also have slip. So the algorithm has to differentiate between when the GPS is

### CHAPTER 3. RESULTS

bad and when the Output-shaft is bad. See A.1 for a pseudo flow-diagram of the algorithm.

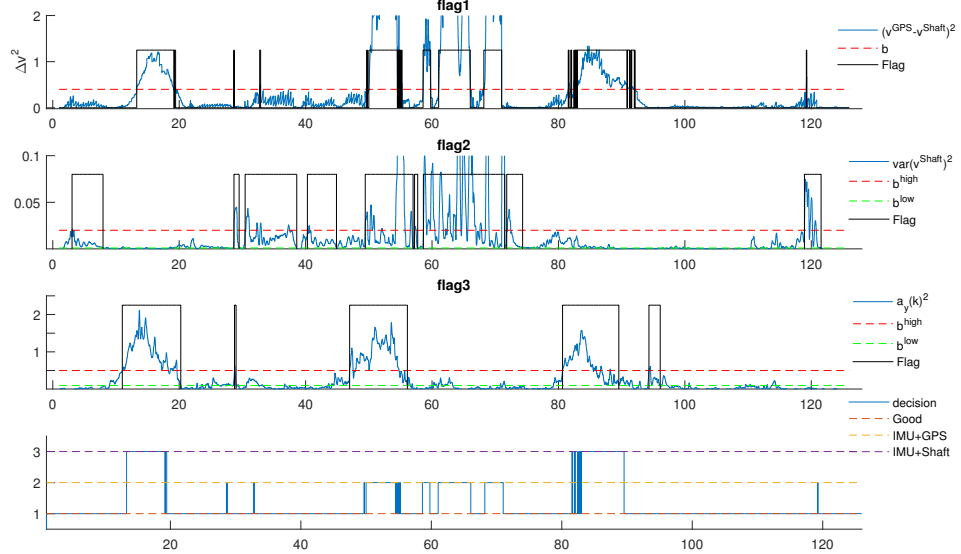


**Figure 3.11.** Shows how the signals used to make a logical decision whether to trust a velocity measurement. Three different flags are used, and atleast two are needed to make a deduction that the signal is either slipping or drifted.

In Figure 3.12 the velocity estimation from the algorithm is shown together with the velocity measurements. The error between the estimated velocity from the proposed algorithm and the "true" velocity from the reference GPS is shown. Slip was also added afterwards during a period where the GPS was good, because otherwise it is obvious that the velocity estimation will be bad.

### 3.4. ROBUSTNESS

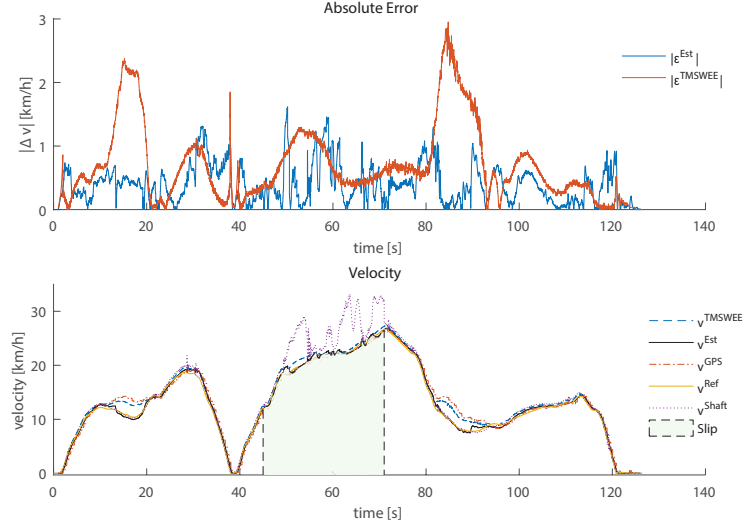


**Figure 3.12.** The top image shows the error between the proposed algorithm and the current velocity estimation in the TMS. The bottom image shows the velocity estimates together with the velocity measurements. Root mean square error of the proposed method: 0.131, TMSWEE: 0.255

#### 3.4.3 Velocity extremes

Because Scania's current method of estimating velocity have issues at the velocity extremes, like high and low speeds, discussed in Section 2.6. The results from both these cases are examined in this section.

##### High velocities

In the longer driving-scenario where the vehicle is subjected to high velocities, TM-SWEE may have an absolute error due to a scaling error. This is displayed in Figure 3.13. The absolute error is plotted in the top image. If compared to the proposed method, it will have a reduced absolute error. This is because the GPS and Output-shaft are fused together, and thus the overall observation of the velocity will inherit the error from the Output-shaft, even though it will be reduced by the accuracy of the GPS. The GPS will not have this absolute error and therefore it is desirable to omit the Output-shaft in these high velocities.

From the Slip-detection algorithms it is easy to add a simple constraint that flags the Output-shaft as bad after certain velocities. The result is displayed in Figure 3.14, there is a clear decrease in the absolute error of the estimation.

If considering the entire drive-scenario the overall RMSE when there is no logic in consideration 0.246 compared to 0.240 when there is.

### CHAPTER 3. RESULTS

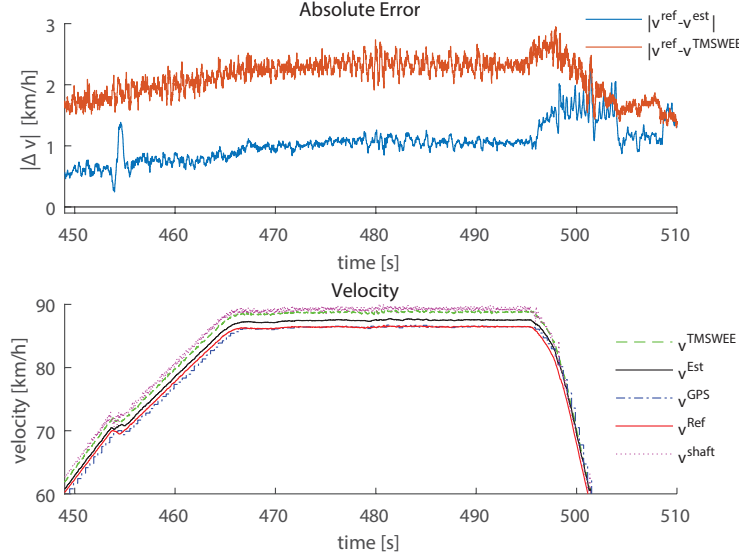


**Figure 3.13.** Top figure contains the absolute error of the proposed method and the current TMSWEE. In the lower image the corresponding velocity-estimate is displayed.

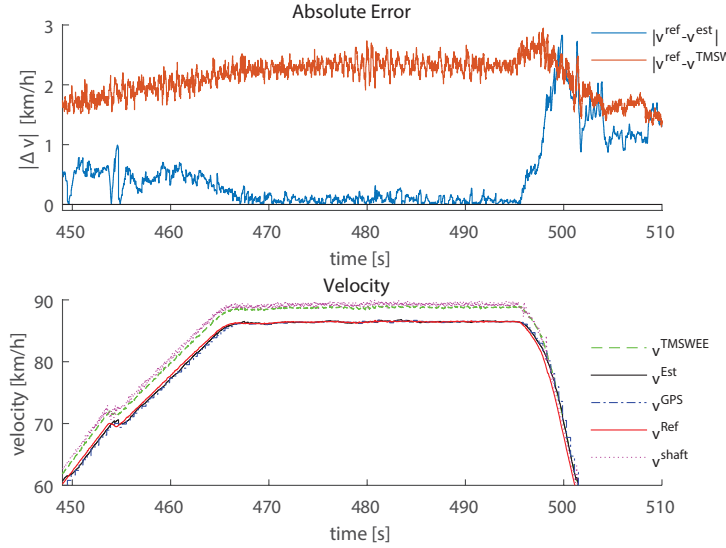


**Figure 3.14.** Top figure contains the absolute error of the proposed method and the TMSWEE. In the lower image the corresponding velocity-estimate is displayed. At fast speeds the Output-shaft will have bad properties due to errors in the scale factor. Because both the GPS and the Output-shaft are accessible one can use a logic constraint to only trust the GPS, thus improving the result.

### 3.4. ROBUSTNESS

#### Low velocities

Low velocities are a very critical scenario when a good estimation is desirable. Because the TMS's velocity estimation is based on the wheel encoders, and have a hysteresis property in this velocity spectrum. Therefore it will not provide a velocity observation after a certain velocity. In Figure 3.15 in the top image the error is displayed. The absolute error is growing until it hits about  $1\text{km/h}$  before decreasing. In the same image the error corresponding to the proposed method is displayed. It shows better performance than the TMSWEE in the lower regions from about  $0 - 2\text{km/h}$  then the estimation deteriorates because of the delay in the GPS signal.

With the same reasoning for the high velocity case, the GPS will have bad properties in the lower velocity region. It is too slow and the delay will make the relative error very large. Therefore, ignoring the GPS at lower velocities will make the overall estimate better. In Figure 3.16 the error with only the velocity-observation from the Output-shaft and the acceleration from the IMU is used.

The error is much smaller compared to the error from when both the GPS and Output-shaft was used. But the TMSWEE out-preforms the proposed method after  $2\text{km/h}$  to about  $15\text{km/h}$ , because the wheel encoders are very accurate in that region. Consider the previous figures for that velocity region. The error in the velocity estimation from the proposed method is below  $0.5\text{km/h}$  throughout that region.

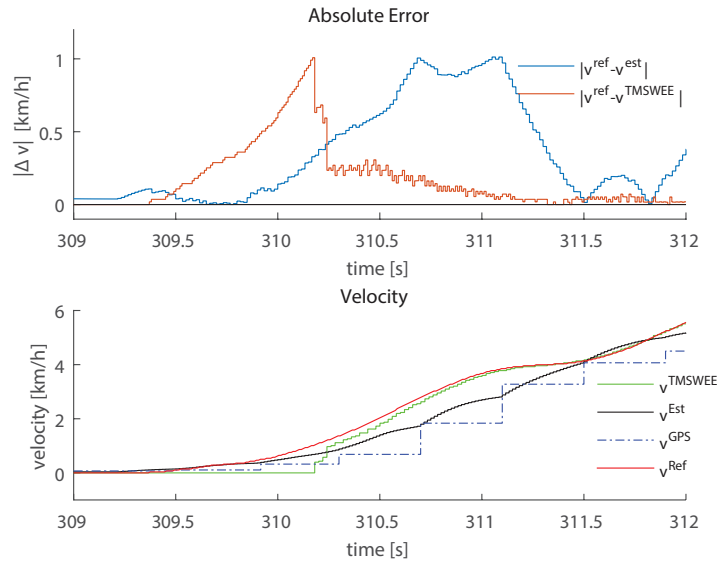


**Figure 3.15.** Top figure contains the absolute error of the proposed method and the current TMSWEE. In the lower image the corresponding velocity-estimate is displayed.

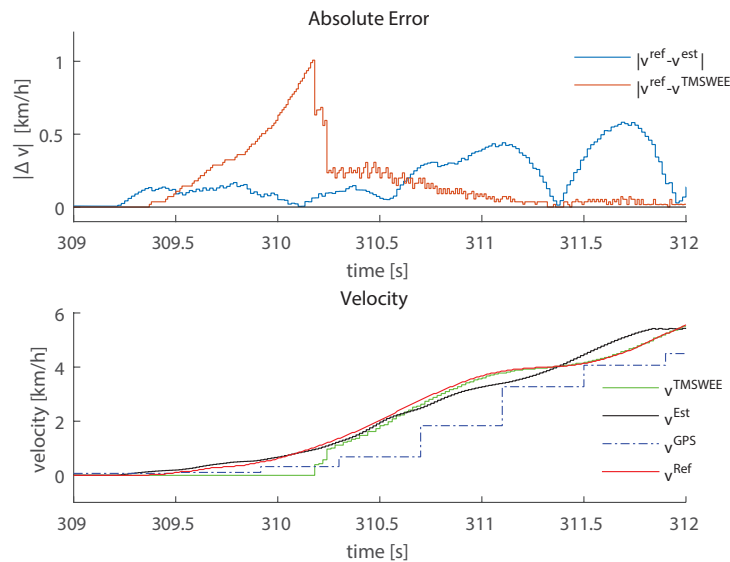


**Figure 3.16.** Top figure contains the absolute error of the proposed method and the current, TMSWEE. In the lower image the corresponding velocity-estimate is displayed. At low speeds the GPS will have bad properties due to latency and low update-frequency. Because the GPS and the Output-shaft are fused together, the fused signal will inherit the delay and therefore have an offset to the true velocity. One can use a logic constraint to only trust the Output-shaft, thus improving the result.

### 3.5. DELAY COMPENSATION

## 3.5 Delay compensation

The delay in the GPS is a serious problem in critical scenarios, low velocities see Section 3.4.3, fast accelerations or deceleration. This leads to rapid deterioration of the estimations accuracy. To obtain accurate estimation with a sensor-configuration with IMU and GPS this will be a big issue. One can either improve the sensor architecture and limit the magnitude of the delay. The other option is to compensate for the delay. In Section 2.8 a method for compensating for the delay was proposed.

In Figure 3.17 the resulting velocity estimation is displayed. In the top image the absolute error between the reference GPS and the corresponding estimates are presented. In the figure a segment of the drive-scenario is presented. From the top figure it is clear that the delay compensation will overall have a lower absolute error compared to both the TMSWEE and the non-compensated.

Because the method is based on measurement extrapolation, the corresponding measurement of the GPS-signal is displayed for a small segment of the scenario in Figure 3.18. In Table 3.5 a compilation of the errors from the scenario is displayed. There is a great improvement in both the RMSE and the MAE, compared to the non-compensated system. The downsides are that in some cases the extrapolation tend to overshoot, thus making the peak error larger than the filter without delay-compensation.

## CHAPTER 3. RESULTS

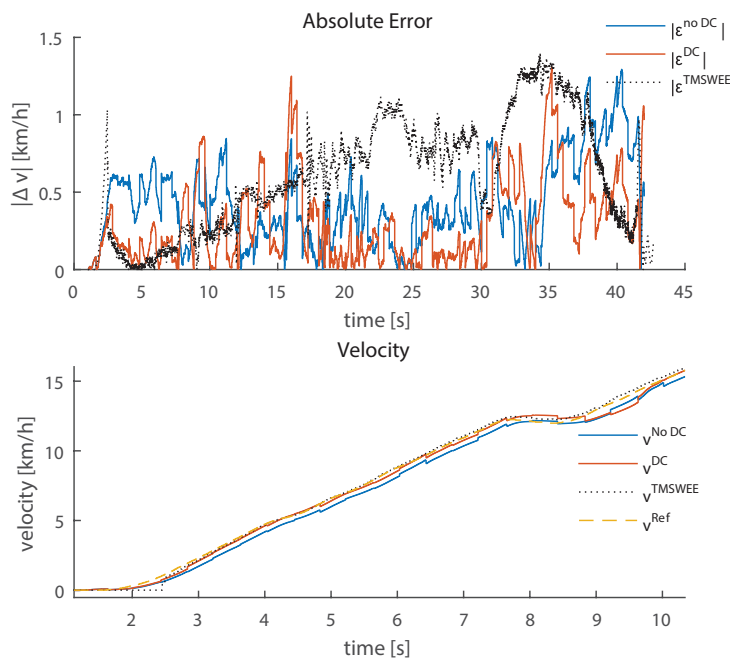


**Figure 3.17.** This image shows the velocity estimation from the driving-scenario where the vehicle is driving up a small hill. To illustrate the improvement of compensating for the latency in the GPS, the Output-shaft is excluded. In the top plot the absolute error from the velocity estimation from the SMO when latency is and is not compensated for. Together with the absolute error from the current TMS's estimation.

### 3.5. DELAY COMPENSATION

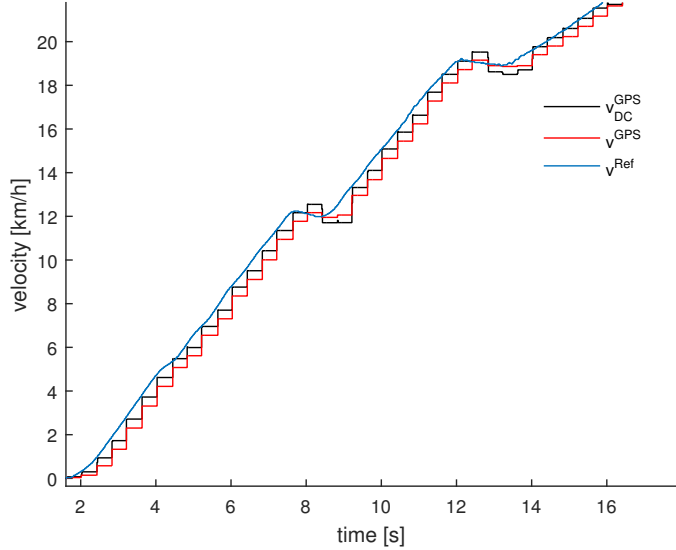


**Figure 3.18.** This image shows the extrapolated GPS measurement, the original GPS-measurement, and the reference GPS-signal. As shown the delay is accurately compensated for. But for fast transient areas the accuracy will vary.

	Without DC	With DC	TMSWEE
<i>RMSE</i>	0.5119	0.4084	0.7062
<i>MAE</i>	0.4317	0.3036	0.5996
<i>Peak Error</i>	1.2936	1.3086	1.4040

**Table 3.5.** This table shows the improvement of the signal when compensating for delay from the GPS signal, with the Sliding mode observer technique. This is obtained from the case of a small hill. Note, this filter is tuned differently compared to the previous filters. Therefore not directly comparable, but proves the benefits of compensating for delay.



## Chapter 4

# Discussion and Conclusion

### 4.1 Discussion

#### Complete sensor configuration

The benefits of having a more complete IMU set-up is that the measurements of the pitch will have a more accurate and high-frequent update. This is important when there is only a IMU+GPS configuration. This configuration is very important because when the Output-shaft starts to slip, IMU+GPS will be the sensors that will provide the velocity estimate. Therefore it is important that the IMU measurements are accurate in-between the GPS samples. See Section 3.3 and Table 3.4. But if the Output-shaft is available as an additional velocity-observation, the overall velocity-estimate will not be as dependent on a good acceleration measurement. Thus the performance will not be greatly impacted, therefore adding a pitch gyro to the TMS is not truly justified. See Figure 3.10.

But when GPS-outage and the Output-shaft is slipping the system has to rely solely on the accelerometer, and if the vehicle is in a hill it is absolutely crucial that the pitch is correct. See Section 3.3.

In Section 3.3.1 the Coriolis effect is explored. This is one of the big benefits in having a more complete sensor configuration that would otherwise be unobservable. By adding a yaw-gyroscope and measuring the difference between the GPS and the Output-shaft the Coriolis could be calculated. This is directly linked to errors measured in the forward directed accelerometer,  $a_x$ . If Coriolis is taken into consideration and corrected for, it will improve estimation of the velocity. See Section 3.3.1. But to measure the Coriolis acceleration both the GPS, Output-shaft and yaw-gyro needs to be measured. If either the Output-shaft or the GPS is lost, Coriolis is unobservable. Like the pitch-gyroscope: if both the GPS and Output-shaft are available, the accuracy of the accelerometer is not crucial. It is therefore not a necessity to have a yaw-gyroscope to provide an accurate velocity estimation.

But there are other benefits that would justify having a yaw-gyro. The Coriolis-effect is the ultimate indication that the GPS is not providing an accurate velocity

## CHAPTER 4. DISCUSSION AND CONCLUSION

estimation, and needs to be excluded in favour of the Output-shaft.

### Filter performance

The overall performance difference between the EKF and SMO is small. But the SMO is slightly better in the scenarios that were evaluated. The reason for that is that the SMO better tuned thus having a smaller RMSE and MAE. Because the two filters are very different it is equally hard to tune them in a manner such that the performance can be compared fairly. But like the literature suggests the SMO will have similar properties to the EKF. Even though it is crude by nature and suboptimal, it will have equal performance, see Section 3.2.

In Section 3.5 a delay-compensation algorithm using SMO is also displayed. The delay is the biggest source of errors in the velocity-observation. So if one wants an accurate and robust velocity estimation the delay has to be dealt with. The algorithm is able to compensate for the delay in the GPS signal, and improve the overall estimate. See Table 3.5 and Figure 3.17. But the parallel delay-compensation filter will have problems with fast changes like breaking, gear-switching and breaking to a full stop. The algorithm will tend to overshoot, and has to be finely tuned. This is a clear area of improvement and has to be investigated further for a more robust solution.

### Logic constraints

The logic constraints used in this project started from the scenario where the Output-shaft slips. With the three flags used, one to detect differences in the velocity, measure the variance of the Output-shaft during a small time-instance, and large magnitudes in  $a_y$ . Slip in both the Output-shaft and GPS could be detected. The key to this algorithm was the first flag that detect differences in the velocity. The only time the GPS-signal will provide a bad estimation is when the vehicle turns rapidly, and the velocity will not deviate much from the true velocity. Therefore the GPS-signal is generally more reliable than the Output-shaft. In the case where all three flags are active, it is better to trust the GPS, than the Output-shaft. In the scenario where the vehicle was turning, the algorithm was able to differentiate between them two. See Figure 3.11 and Figure 3.12. This algorithm was able to perform better than TMSWEE even with these large errors in the observations. But this scenario was on a flat surface, and it might be interesting to evaluate a scenario where the vehicle is turning while driving in a slope.

Logic constraints were also useful during velocity extremes, low and high velocities. Because the GPS is more accurate than the Output-shaft at high velocities due to the scaling-factor error present in the Output-shaft the signal is omitted at high velocities. Similarly the GPS, at low velocities is inaccurate due to the low update-frequency and delay, thus there is a clear benefit to ignore the GPS-signal. The

## 4.2 CONCLUSION

result is showed in Figure 3.14 and Figure 3.16. Similar results could be achieved in the fusing of the velocity estimate, Equation (2.40). The covariance for the GPS and Output-shaft could be changed as a function of the velocity. This would give a smother transition between trusting only the GPS and vice-versa.

## 4.2 Conclusion

It is possible with a GPS and the current TMS's internal signals to obtain an accurate velocity estimation. The minimal sensor-configuration Output-shaft, GPS, and the 2-axis IMU is able to provide an accurate velocity, and pitch estimate. Better than the current velocity estimate from the TMS, based on wheel-encoders from the scenarios considered in this project. This sensor fusion was achieved with two different state-observers: Sliding mode observer and an extended Kalman filter. Either one of the filters will provide an accurate estimate, but there are certain computational benefits with the Sliding mode observer.

However expanding the sensor-configuration with gyroscopes measuring both pitch and yaw angular-velocity respectively will make the overall estimation better. The pitch gyro will be able to update and maintain an more accurate pitch estimate in between the GPS-samples. Which will in critical scenarios, like hills, prevent drift in the velocity-estimate due to integration of gravity induced errors affecting the accelerometers. Similarly the yaw gyroscope together with the velocity difference between the GPS and Output-shaft can observe the Coriolis-acceleration experienced by the accelerometer in the forward direction. Compensating for this acceleration will improve the estimate. The Coriolis-acceleration is also the ultimate indicator when the GPS-signal experiences slip. Because a yaw-gyro sensor-configuration is not available in the TMS, an alternative indicator based on the accelerometer in the side direction was used to observe GPS-slippage. A method based on logical-constraints was created to indicate when a signal started to slip. Based on velocity differences between the Output-shaft, variances in a small time-increment of the Output-shaft, and the acceleration in the side-direction, the algorithm was able to deduce which of the velocity signals slipped and the bad signal was omitted. The logical constraints was then expanded to exclude the GPS at low velocities and the Output-shaft at high velocities, where these observations are bad and impairs the estimate. Another major sources of error are associated with delay in the GPS-signal. This was compensated for with a method using a parallel filter based on the Sliding mode observer and extrapolation of the GPS-measurement.

## 4.3 Future work and recommendations

- In this project all the algorithms were performed offline on saved data from different driving-scenarios. Thus implementing these proposed methods in a real vehicle and running them in real-time observing the behaviour. This would however require some changes to the sensor architecture in the CAN-network

## CHAPTER 4. DISCUSSION AND CONCLUSION

and the communication between the control-units. The internal communication would have to relay the GPS signal at the highest possible update-frequency of  $5Hz$  to CAN. But also send important down-velocity in the NED coordinate-system, such that the pitch-observation from the GPS can be obtained. Currently, only the vehicle-speed is sent over the CAN-network.

- Look at more cases, i.e sharp turns in hills. In this scenario the vehicle would most likely have slip in the Output-shaft and the GPS [1]. Therefore the logical-constraints might need revision. All the algorithms would have to be evaluated in more detail to obtain an as robust tuning and constraints, but this would require more data.
- Investigate the minimal accuracy needed for Opticruise to operate. Currently no such information is available. The accuracy is most likely velocity dependent, where the vehicle has rapid gear switches and thus important to have a very good velocity measurement. This is important to investigate.

# Bibliography

- [1] <http://www.scania.com/group/en/section/about-scania/>, and contact on Scania. Refer to Agnes Johansson, personal conversation 12 April 2016.
- [2] Torkel Glad and Lennart Ljung, *Control Theory - Multivariable and Nonlinear Methods*, Taylor and Francis, New York, 2000.
- [3] Fredrik Gustavsson, *Statistical Sensor Fusion*, page. 30-31, Studentlitteratur, Lund, 2010.
- [4] Sukkarieh, S. (2000). Low Cost, High Integrity, Aided Inertial Navigation Systems for Autonomous Land Vehicles. The University of Sydney.
- [5] Bevly, D. M. (2004). Global Positioning System (GPS): A Low-Cost Velocity Sensor for Correcting Inertial Sensor Errors on Ground Vehicles. Journal of Dynamic Systems, Measurement, and Control. <http://doi.org/10.1115/1.1766027>
- [6] Jarrell, J., Gu, Y., Seanor, B., & Napolitano, M. R. (2008). "Aircraft Attitude, Position, and Velocity Determination Using Sensor Fusion". Proceedings of the AIAA Guidance, Navigation, and Control Conference and Exhibit.
- [7] Ribeiro, M. I. (2004)." Kalman and Extended Kalman Filters : Concept , Derivation and Properties". Institute for Systems and Robotics Lisboa Portugal, (February), 42. <http://doi.org/10.1.1.2.5088>
- [8] Saadeddin, K., Abdel-Hafez, M. F., & Jarrah, M. A. (2014). Estimating Vehicle State by GPS/IMU Fusion with Vehicle Dynamics. Journal of Intelligent & Robotic Systems. <http://doi.org/10.1007/s10846-013-9960-1>
- [9] Niu, X., Nasser, S., Goodall, C., & El-Sheimy, N. (2007). "A Universal Approach for Processing any MEMS Inertial Sensor Configuration for Land-Vehicle Navigation". Journal of Navigation, 60(02), 233. <http://doi.org/10.1017/S0373463307004213>
- [10] Zhao, L., & Liu, Z. (2014). Vehicle State Estimation with Friction Adaptation for Four-Wheel Independent Drive Electric Vehicle, 2014(61104060), 4518-4522.

## BIBLIOGRAPHY

- [11] Wu, Y. (2014). Versatile land navigation using inertial sensors and odometry: Self-calibration, in-motion alignment and positioning. 2014 DGON Inertial Sensors and Systems, ISS 2014 - Proceedings, 1-9. <http://doi.org/10.1109/InertialSensors.2014.7049412>
- [12] Engineering, G. (2004). UCGE Reports INS / GPS Integration Using Neural Networks for Land Vehicular Navigation Applications. UCGE Reports Number 20209, (20209).
- [13] Goodall, C. L. (2009). Improving Usability of Low-Cost INS/GPS Navigation Systems by Intelligent Techniques, (20276).
- [14] Flenniken IV, W. S., Wall, J. H., & Bevly, D. M. (2005). Characterization of Various IMU Error Sources and the Effect on Navigation Performance. Ion Gnss 2005, 967-978.
- [15] Shin, E.-H. (2005). Estimation techniques for low-cost inertial navigation. ProQuest Dissertations and Theses, NR06960(20219), 206-206 p. Retrieved from url<http://search.proquest.com/docview/305029321>?
- [16] Larsen, T. D., Andersen, N. a., Ravn, O., & Poulsen, N. K. (1998). Incorporation of time delayed measurements in a discrete-time Kalman filter. Proceedings of the 37th IEEE Conference on Decision and Control (Cat. No.98CH36171), 4(December), 3972-3977. <http://doi.org/10.1109/CDC.1998.761918>
- [17] Van der Merwe, R., Wan, E., & Julier, S. J. (2004). Sigma-Point Kalman Filters for Nonlinear Estimation and Sensor-Fusion: Applications to Integrated Navigation. AIAA Guidance, Navigation, and Control Conference and Exhibit, 1-30. <http://doi.org/10.2514/6.2004-5120>
- [18] Jenkins, B., & Thein, M.-W. L. (2012). "On-board and/or ground-based gyroless accelerometer calibration with uncertain spacecraft inertia for NASA's Magnetospheric MultiScale (MMS) Mission". American Control Conference (ACC), 2012, 185-190. <http://doi.org/10.1109/ACC.2012.6315631>
- [19] Frikha, S., Djemel, M., & Derbel, N. (2010). Observer based adaptive neuro-Sliding mode control for MIMO nonlinear systems. International Journal of Control, Automation and Systems, 8(2), 257-265. <http://doi.org/10.1007/s12555-010-0211-y>
- [20] Thein, M.-W. L. (2002). A discrete time variable structure observer with overlapping boundary layers. Proceedings of the 2002 American Control Conference (IEEE Cat. No.CH37301), 4, 2633-2638. <http://doi.org/10.1109/ACC.2002.1025183>
- [21] Mihoub, M., Nouri, A. S., & Abdennour, R. Ben. (2010). A chattering free second order discrete Sliding mode observer : an experimentation on a chemical reactor, (3),0 739-744.

- [22] Veluvolu, K. C., Pavuluri, S., Soh, Y. C., Cao, W., & Liu, Z. Y. (2006). Observers with multiple sliding modes for uncertain linear MIMO systems. 2006 1st IEEE Conference on Industrial Electronics and Applications, (4), 6-11. <http://doi.org/10.1109/ICIEA.2006.257329>
- [23] "Sliding mode Observer for Vehocle Velocity Estimation with Road Grade and Bank angles" Modify the Reference
- [24] Pettersson, M. (1997). Driveline Modeling and Control. Dissertation No. 484. Linköping University, Linköping.
- [25] Liu, X., & Goldsmith, A. (2004). Kalman filtering with partial observation losses. Proceedings of the IEEE Conference on Decision and Control, 4, 4180-4186. <http://doi.org/10.1109/CDC.2004.1429408>



# Appendix A

## Figures

### A.1 Logic constraints

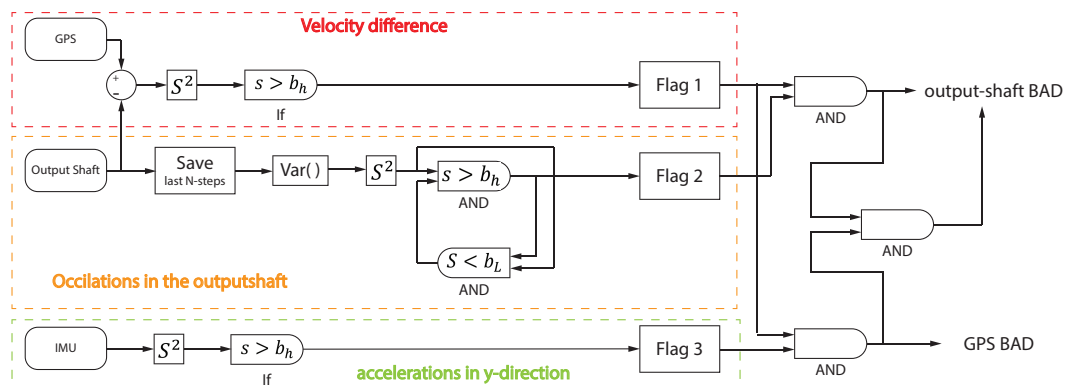


**Figure A.1.** This image is created to illustrate the algorithm for how to determine if the GPS or the Output-shaft is slipping. In the velocity difference box, the if box sees if the velocity is above a certain value of a boundary  $b_h$ . Same in the acceleration in y-direction box. In Oscillation in the Output-shaft, the loop is representing that when the flag 2 is active, it is active until it is below another boundary  $b_L$ .

## A.2 Coriolis

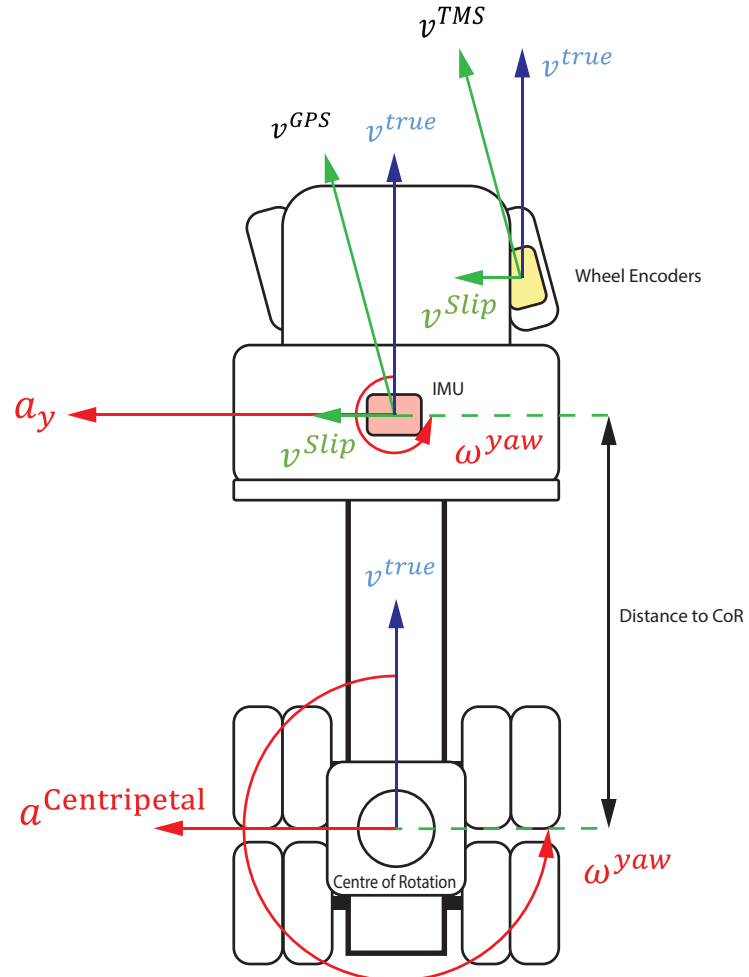


**Figure A.2.** This image is created to illustrate where the velocity difference, between the true and measured velocity from both TMSWEE and the GPS, due to the effect of rotation around the center of rotation (CoR).

# Appendix B

## Code

In this appendix the most important code of two filters are displayed.

**Code B.1.** Code of the prediction and correction step in Sliding mode observer algorithm

```
1 function [ xhat ] = slidingMode( ...
    xhat,f,h,u,y,K_linear,K_switch,limit )
2 % Prediction
3 xhat = f(xhat,u);
4 y_err = y-h(xhat);
5 % Measurement update
6 xhat = xhat + K_linear * y_err+K_switch*sat(y_err,limit);
7 end
```

**Code B.2.** Code of the prediction and correction step in the Extended Kalman filter algorithm

```
1 function [ xhat,P,K ] = EKF( xhat,P,f,h,df,dH,Q,R,u,y )
2 % Prediction
3 xhat = f(xhat,u);
4 P = df(xhat,u)*P*df(xhat,u) '+Q;
5 % Update
6 Sk = dH(xhat)*P*dH(xhat) '+R;
7 K = P*dH(xhat)'*inv(Sk);
8 err = y-h(xhat);
9 xhat = xhat + K * err;
10 P = P - K * dH(xhat) * P;
11 end
```





TRITA -MAT-E 2016:31  
ISRN -KTH/MAT/E--16/31--SE